COOPERATIVE PHENOMENA FOR NEW COHERENT RADIATION SOURCES

R.A. McFarlane

Hughes Research Laboratories
3011 Malibu Canyon Road
Malibu, California 90265

October 1988

F49620-85-C-0058

Final Report

14 May 1987 through 14 June 1988

U.S. AIR FORCE OFFICE OF SCIENTIFIC RESEARCH
Bolling Air Force Base
Washington, DC 20332-6448

UNCLASSIFIED
SECURITY CLASSIFICATION OF THIS PAGE

REPORT DOCUMENTATION PAGE

Form Approved OMB No. 0704-0188

1a. REPORT SECURITY CLASSIFICATION: Unclassified	1b. RESTRICTIVE MARKINGS
2a. SECURITY CLASSIFICATION AUTHORITY	3. DISTRIBUTION / AVAILABILITY OF REPORT: Approved for public release; distribution unlimited.
2b. DECLASSIFICATION / DOWNGRADING SCHEDULE	
4. PERFORMING ORGANIZATION REPORT NUMBER(S)	5. MONITORING ORGANIZATION REPORT NUMBER(S): AFOSR-TR- 89-0321
6a. NAME OF PERFORMING ORGANIZATION: Hughes Research Laboratories; 6b. OFFICE SYMBOL (If applicable)	7a. NAME OF MONITORING ORGANIZATION: Air Force Office of Scientific Research
6c. ADDRESS (City, State, and ZIP Code): 3011 Malibu Canyon Road, Malibu, CA 90265	7b. ADDRESS (City, State, and ZIP Code): Building 410, Bolling Air Force Base, DC 20332-6448
8a. NAME OF FUNDING / SPONSORING ORGANIZATION: Same as 7a; 8b. OFFICE SYMBOL (If applicable): NP	9. PROCUREMENT INSTRUMENT IDENTIFICATION NUMBER: F49620-85-C-0058
8c. ADDRESS (City, State, and ZIP Code): Building 410, Bolling Air Force Base, DC 20332-6448	10. SOURCE OF FUNDING NUMBERS: PROGRAM ELEMENT NO. 61102F; PROJECT NO. 2301; TASK NO. A1; WORK UNIT ACCESSION NO.

11. TITLE (Include Security Classification)

COOPERATIVE PHENOMENA FOR NEW COHERENT RADIATION SOURCES (U)

12. PERSONAL AUTHOR(S)

McFarlane, R.A.

13a. TYPE OF REPORT	13b. TIME COVERED	14. DATE OF REPORT (Year, Month, Day)	15. PAGE COUNT
Final	FROM 5-14-85 TO 6-14-88	1988 October	40

16. SUPPLEMENTARY NOTATION

17. COSATI CODES		
FIELD	GROUP	SUB-GROUP

18. SUBJECT TERMS (Continue on reverse if necessary and identify by block number)

Upconversion lasers, Cooperative phenomena, Pair processes, Rare earth ions, Solid state lasers, Coherent sources, Yttrium lithium fluoride, Erbium (YAG)

19. ABSTRACT (Continue on reverse if necessary and identify by block number)

The principal objective of this research is to investigate, both theoretically and experimentally, cooperative optical transitions in solids, with the goal of finding efficient systems for the generation of upconverted stimulated emission. Of interest also are new optical pair effects and studies of the resonance fluorescence and coherence on cooperative transitions. In the third year of the program, significant advances were made in the experimental aspects. Measurements of upconversion dynamics were made in erbium-doped crystals and in a fluorozirconate glass. Upconversion laser operation was observed at two visible wavelengths in $YLiF_4$:Er 5% and pumping pathways identified. Spectral and lifetime studies are reported for promising new laser host materials.

20. DISTRIBUTION / AVAILABILITY OF ABSTRACT: ☐ UNCLASSIFIED/UNLIMITED ☒ SAME AS RPT. ☐ DTIC USERS	21. ABSTRACT SECURITY CLASSIFICATION: Unclassified
22a. NAME OF RESPONSIBLE INDIVIDUAL: H.R. Schlossberg	22b. TELEPHONE (Include Area Code): 202/767-4906; 22c. OFFICE SYMBOL: NP

DD Form 1473, JUN 86 — Previous editions are obsolete.

SECURITY CLASSIFICATION OF THIS PAGE

UNCLASSIFIED

TABLE OF CONTENTS

SECTION		PAGE
1	RESEARCH OBJECTIVES	1
2	PUMP LASER SOURCES AND SPECTROSCOPY	3
	2.1 Pump Lasers	3
	2.2 Spectroscopy	3
3	LASER EXPERIMENTS	17
	3.1 Pulsed Pump Excitation - 1.54 μm	17
	3.2 CW Pump Excitation - 791 nm	20
4	NEW MATERIALS AND DIRECTIONS	27
	APPENDIX A	A-1
	LIST OF PUBLICATIONS AND PRESENTATIONS	P-1
	REFERENCES	R-1

LIST OF ILLUSTRATIONS

FIGURE		PAGE
1	1.54 μm Raman-Shifted Laser Pulse	4
2	Energy Levels of the Erbium Ion	5
3	Energy Levels and Pumping Scheme of the Er:$LiYF_4$ Upconversion Laser	7
4	Time Dependence of Upconverted Emission of CaF_2 Excited by 1.54 μm, 10 ns Pulse	9
5	Early Time Dependence of Upconverted Emission of CaF_2 Excited by 1.54 μm, 10 ns Pulse	10
6	Early Time Approach to Maximum Population of $^4I_{11/2}$ Level	12
7	1.54 μm Emission from BaY_2F_8:Er 5%	14
8	1.54 μm Emission from BaY_2F_8:Er 5%	15
9	Temperature Dependence of Fluorescence from $YLiF_4$:Er 5% from the $^4S_{3/2}$ and $^4F_{9/2}$ Levels for 1.54 μm Excitation	21
10	551-nm Output Pulse Train	21
11	Build-up of cw Laser Output at 671 nm	23
12	671-nm Output Modulation Occurring When 551 nm Transition is Simultaneously Present	25
13	Variation of 671 nm Laser Output With Pump Power Above Threshold	25
14	Extinction Coefficient for BaY_2F_8:Er 5%	28
15	Extinction Coefficient for BaY_2F_8:Er 5% at the $^4I_{15/2} \rightarrow {}^4I_{9/2}$ Pump Band	28
16	Extinction Coefficient for BaY_2F_8:Er 5% at the $^4I_{15/2} \rightarrow {}^4I_{13/2}$ Pump Band	30
17	Decay of $^4I_{13/2}$ in BaY_2F_8:Er 5% Under Short Pulse UV Excitation	30

LIST OF ILLUSTRATIONS

FIGURE		PAGE
18	Logarithmic Decay of $^4I_{13/2}$ in BaY_2F_8:Er 5% Under Short Pulse UV Excitation.....	31
19	Decay of $^4I_{11/2}$ in BaY_2F_8:Er 5% Under Short Pulse UV Excitation.....	31
20	Logarithmic Decay of $^4I_{11/2}$ in BaY_2F_8:Er 5% Under Short Pulse UV Excitation.....	32
21	Extinction Coefficient for $YErLiF_4$:Ho 0.5%.....	32
22	Extinction Coefficient for $YErLiF_4$:Ho 0.5% at the $^4I_{15/2} \rightarrow {}^4I_{9/2}$ Pump Band.....	33
23	Extinction Coefficient for ErF_3.....	35
24	Extinction Coefficient for ErF_3 at the $^4I_{15/2} \rightarrow {}^4I_{9/2}$ Pump Band.....	35
25	Extinction Coefficient for CaF_2:Er 5%.....	A-2
26	Extinction Coefficient for CaF_2 at the $^4I_{15/2} \rightarrow {}^4I_{9/2}$ Pump Band.....	A-2
27	Extinction Coefficient for CaF_2 at the $^4I_{15/2} \rightarrow {}^4I_{13/2}$ Pump Band.....	A-3
28	Extinction Coefficient for $YLiF_4$:Er 5%.....	A-3
29	Extinction Coefficient for $YLiF_4$:Er 5% at the $^4I_{15/2} \rightarrow {}^4I_{9/2}$ Pump Band.....	A-4
30	Extinction Coefficient for $YLiF_4$:Er 5% at the $^4I_{15/2} \rightarrow {}^4I_{13/2}$ Pump Band.....	A-4
31	Extinction Coefficient for ZBLAN:Er 4%.....	A-5
32	Extinction Coefficient for ZBLAN:Er 4% at the $^4I_{15/2} \rightarrow {}^4I_{9/2}$ Pump Band.....	A-5
33	Extinction Coefficient for ZBLAN:Er 4% at the $^4I_{15/2} \rightarrow {}^4I_{13/2}$ Pump Band.....	A-6

PREFACE

This is the third and final report describing an investigation of radiative transitions of coupled pairs of atoms and ions for application to new sources of coherent radiation. The final year of the program has emphasized studies of rare-earth-doped crystals and glasses exhibiting cooperative interactions, whereby it is possible to obtain laser emission in these systems at wavelengths shorter than those at which they are excited.

Participating in this research program during the final year were the following personnel: R.A. McFarlane as principal investigator, S.A. Pollack for a portion of the upconversion laser measurements, J.F. Lam for theoretical studies, with technical assistance provided by R.A. Cronkite.

This research is being supported by the U.S. Air Force Office of Scientific Research, Bolling AFB, D.C. The program is under the technical supervision of Dr. Howard Schlossberg, Physics Directorate.

SECTION 1

RESEARCH OBJECTIVES

During the final year of this program, as guided by discussions with the Air Force Office of Scientific Research technical monitor, Dr. Howard Schlossberg, we established the technical objective of identifying specific candidates for operation of an upconversion laser based on erbium-doped crystals or related glasses was established. This required spectroscopic studies of the several candidates being considered, development of the necessary IR laser sources required for excitation of particular states of the erbium ion, measurements of the resulting near-IR, visible, and UV spontaneous emission to demonstrate that upconversion processes were operative, and finally, the establishment of laser operation in promising hosts.

Section 2.1 discusses the two laser sources employed in this study. The first was used to excite the $^4I_{13/2}$ level of the Er^{3+} ion in the several hosts studied at a wavelength of 1.54 μm and operated in a pulsed mode. The second pump laser operated at 791 nm and was used to excite the $^4I_{9/2}$ level of the Er^{3+} ion.

During this third portion of the program, several hosts were evaluated. Detailed absorption measurements were made over the range of wavelengths from 3000 Å to 1.6 μm; fluorescence observations established that upconversion pumping was providing excitation of not only ionic levels requiring the energy of two incident photons, but of three and four photons as well; and finally, the time dependencies of the level populations were recorded to determine radiative lifetimes. Cooperative excitation processes were apparent from the nonexponential decays of the excited levels, particularly the $^4I_{13/2}$ at 1.54 μm, and from the very long time duration of emission from

cooperatively excited higher lying levels. The details of these measurements are reviewed in Section 2.2.

Promising new crystals include erbium-doped $YLiF_4$, which has recently been operated in the upconversion pumping mode in the IR by S.A. Pollack of Hughes, and at 551 nm by researchers at IBM. It is in this material that we have established cw upconversion operation at 671 nm, as reported in Section 3. We have also observed simultaneous 551 nm operation. This section summarizes a series of laser experiments conducted with both 791 nm and 1.54 μm pump sources.

Other materials on which we have initiated measurements, in addition to CaF_2 as host, include Hughes Research Labs-grown BaY_2F_8 and ZBLAN fluorozirconate glass. The latter material has been operated recently as a 2.7 μm laser using upconversion pumping at 1.54 μm.[1]

Section 4 discusses new host crystals and cites examples of high doping density systems.

Appendix A summarizes absorption data taken on the materials on which laser experiments were undertaken during the final year of this program.

SECTION 2

PUMP LASER SOURCES AND SPECTROSCOPY

2.1 PUMP LASERS

The pump laser employed for the 2.7 μm experiments reported in our last annual report was an Er:glass laser operating at 1.53 μm in a long pulse mode (~1 ms) at a repetition rate of one pulse-per-minute. To facilitate more rapid spectral data collection, a 10 pps Quanta Ray DCR-2 Nd:YAG laser was used to drive a 1 m methane cell in a double pass geometry to produce Raman-shifted output at 1.54 μm. Pulse energy of 40 mJ was obtained. Figure 1 shows the 10 ns time dependence, essentially a replica of the 1.06 μm Nd:YAG Q-switched output.

To provide cw pumping of the laser rods under study, we employed a Coherent Model 699 dye laser, pumped by a Coherent Model CR18 argon ion laser. Using laser dye LDS 751, the system provided 300 mW at the required pump wavelength of 791 nm. The exact wavelength required was determined from detailed spectral absorption measurements, which are displayed for the several host crystals in Appendix A. A Burleigh Model WA-20 wavemeter provided precise calibrations for setting the dye laser wavelength.

2.2 SPECTROSCOPY

The energy levels of the erbium ion are shown in Figure 2. Because erbium has fully filled 5s and 5d shells, but a partially filled 4f shell that is responsible for the observed optical transitions, its spectroscopic properties are only slightly affected by local crystal fields. Consequently, a variety of hosts, both crystals and glasses, give similar absorption and emission features. As we will see later, small differences in linewidths and relative line intensities are

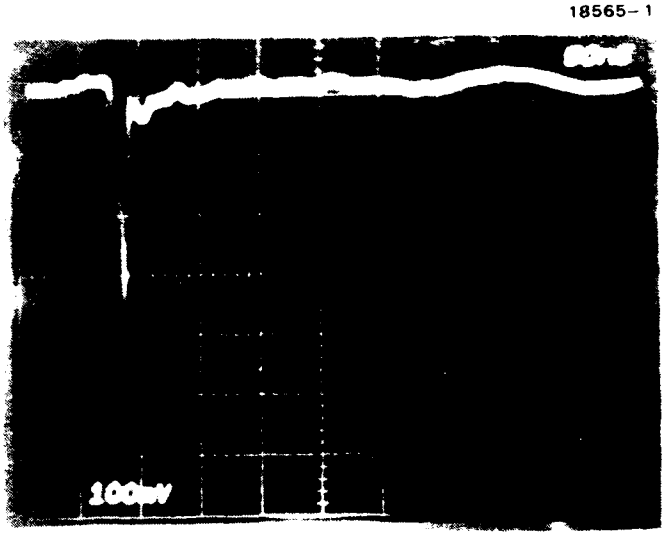

FIGURE 1. 1.54 μm Raman-shifted laser pulse. Scale 50 ns cm^{-1}.

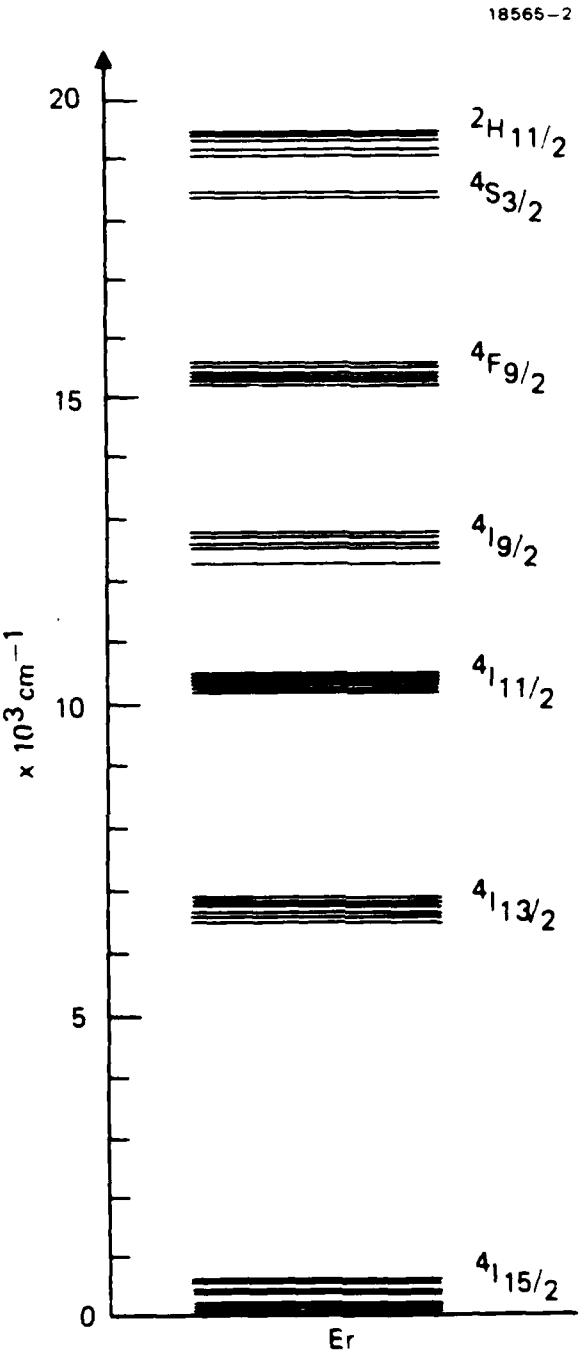

FIGURE 2. Energy levels of the erbium ion.

found, particularly in glass hosts, and in instances where charge-compensating defects influence the site symmetry of the erbium ion.

The present work addresses the pumping of the $^4I_{13/2}$ level at 1.54 μm and the $^4I_{9/2}$ level at 791 nm. As discussed in the previous annual report, excitation at 1.54 μm gives rise to "upconversion pumping," which exploits the sharing of the energy of two $^4I_{13/2}$ ions to produce one ion in the $^4I_{9/2}$ level and one in the ion ground state. As shown in Figure 3, this has resulted in laser emission at 2.7 μm following the population of the $^4I_{11/2}$ upper laser level by rapid decay from the $^4I_{9/2}$ level. The transition $^4I_{11/2} \rightarrow {}^4I_{15/2}$ at 0.98 μm should represent a second candidate for upconversion laser operation and was the initial objective of this final year study.

When the Raman 1.54 μm source was used to excite a variety of the erbium-doped samples, the time dependence of spontaneous emission was measured at wavelengths corresponding to a number of higher lying states of the ion (Table 1).

Table 1. Upconverted Emission Systems.

Wavelength	State
985 nm	$^4I_{11/2}$
828 nm	$^4I_{9/2}$
671 nm	$^4F_{9/2}$
551 nm	$^4S_{3/2}$
410 nm	$^2H_{9/2}$
382 nm	$^4G_{11/2}$

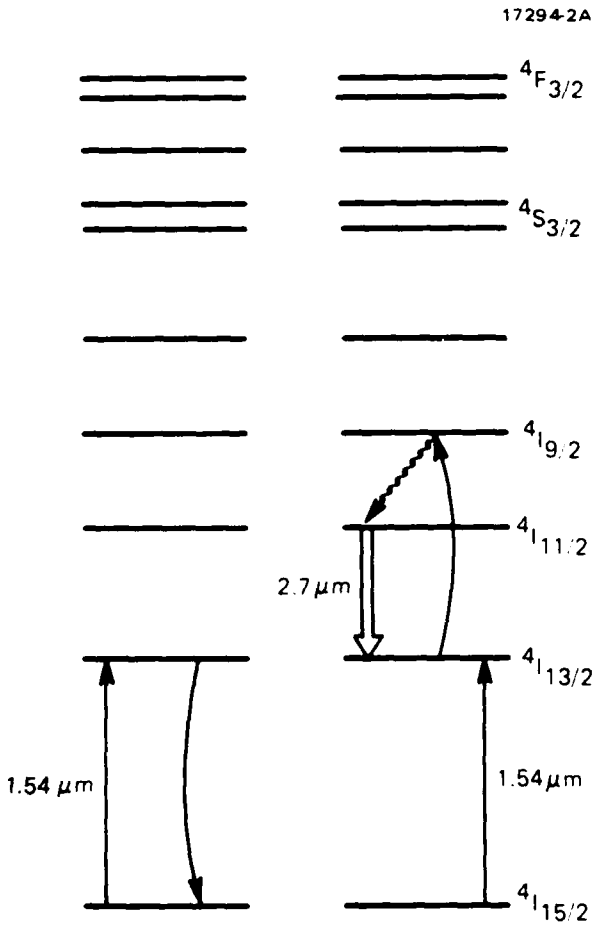

FIGURE 3. Energy levels and pumping scheme of the Er:$LiYF_4$ upconversion laser. Pumping wavelength is at λ = 1.54 μm (Er:glass laser) and laser action occurs at ~2.7 μm due to pair upconversion alone.

The samples examined were CaF_2:Er 5%, $YLiF_4$:Er 5%, BaY_2F_8:Er 5%, and ZBLAN:Er 4%. The last is a fluorozirconate glass that has been employed as a host for mid-IR laser operation.[1] The results for CaF_2 are presented in Figure 4, which show the late time behavior of the upconversion emission from the above energy levels. The long decay times do not represent the true radiative or nonradiative decay times of the states being observed, since these are typically orders of magnitude smaller. Rather, what is observed is the upconversion process itself as energy is shared among the lower energy levels to populate higher lying states. The present experiment differs from earlier measurements that (1) use short wavelength excitation to study the upconversion dynamics by examining the deviation from single exponential decay of any level as energy migrates down the energy level ladder,[2] or (2) observation of anti-Stokes emission resulting from energy migration within a pair or triad.[3]

The complete characterization of the present system that has so many coupled levels (at least eight) is extremely complex. A rate equation analysis including cross relaxation coefficients has been discussed by W. Shi[4] for short wavelength excitation, and a similar analysis should be applicable here. A critical determination of initial populations must be made in order to use such an analysis. From the very early time data shown in Figure 5, for the levels studied here, the populations build up over a period lasting several microseconds to several hundred microseconds. This suggests that simultaneous multiple photon absorption of 1.54 μm pump energy is not a direct major contributor to these initial level populations, since our instrumentation would have detected signal risetimes much less than 100 ns. The rapid build-up of population in the $^4G_{11/2}$, $^2H_{9/2}$, $^4S_{3/2}$, and $^4I_{9/2}$ levels is not inconsistent, however, with rapid radiative or nonradiative decay into these states from some as-yet undetermined higher level excited through

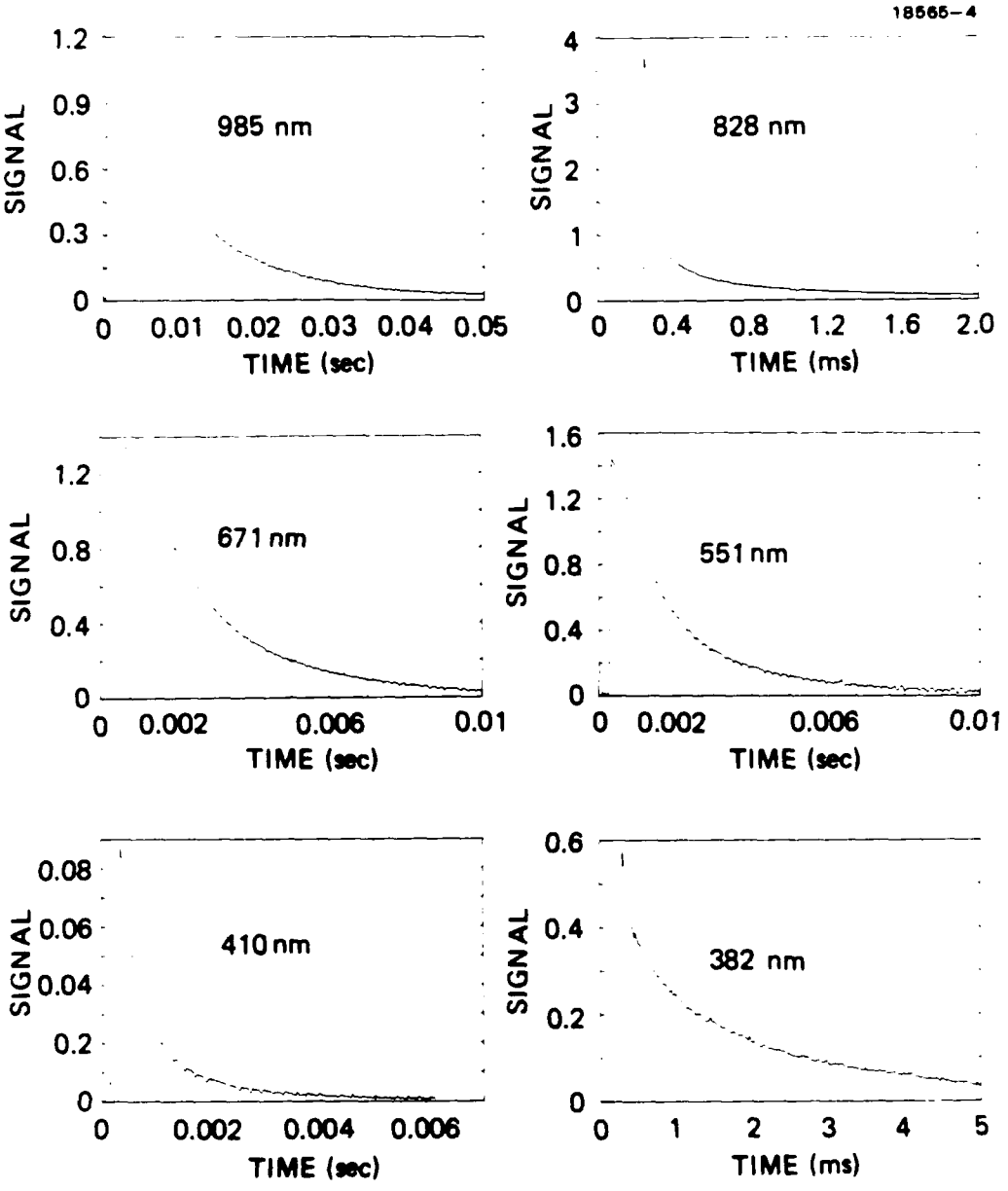

FIGURE 4. Time dependence of upconverted emission of CaF_2 excited by 1.54 μm, 10 ns pulse. Trigger point differs for each trace.

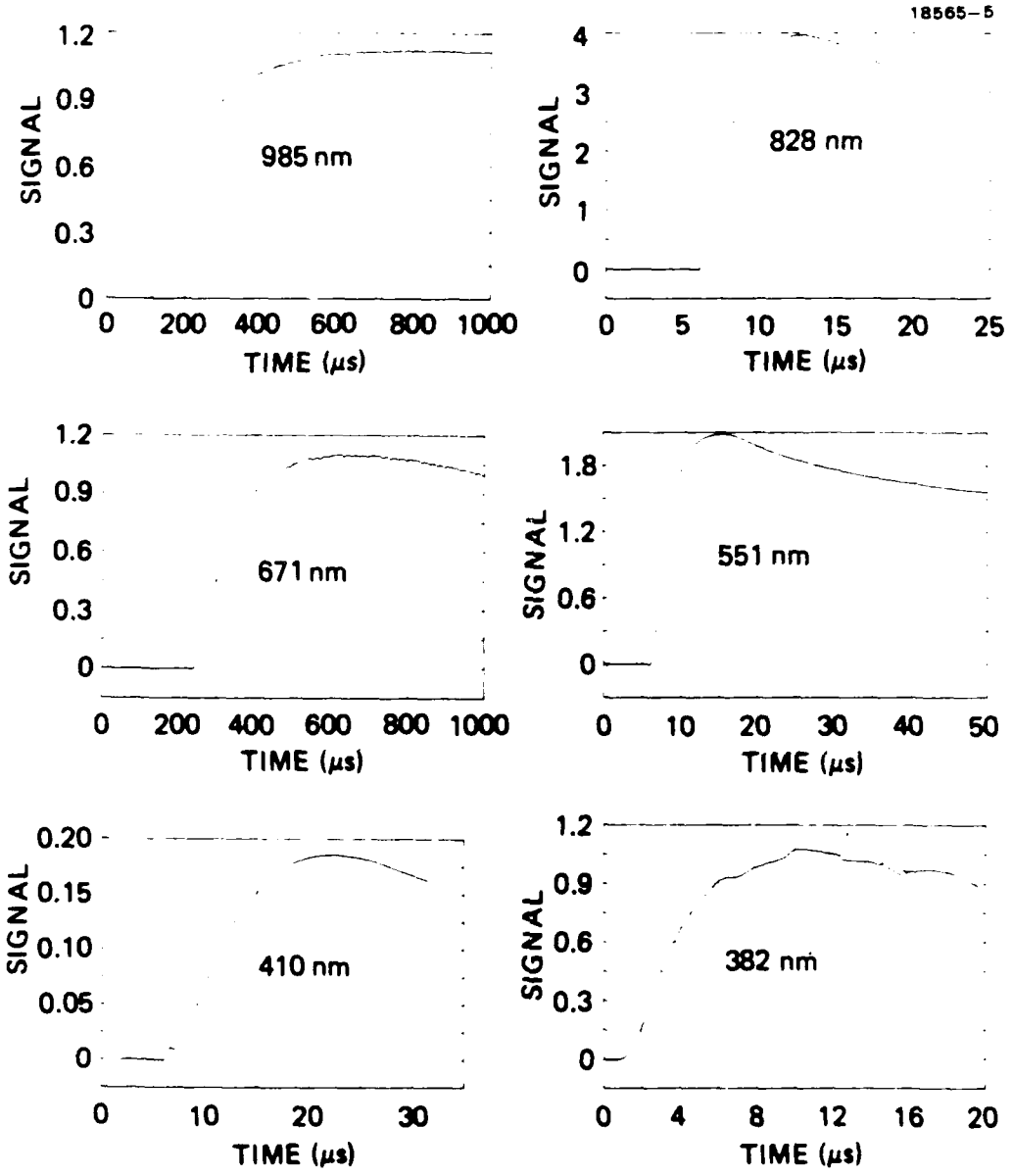

FIGURE 5. Early time dependence of upconverted emission of CaF_2 excited by 1.54 μm, 10 ns pulse. Trigger point differs for each trace.

multiphoton processes. Failing this, the rapid appearance of these states subsequent to 1.54 μm excitation requires that very efficient upconversion energy pooling be taking place.

It is not possible to infer from the risetime data of Figure 5 the decay lifetime of the undetermined level, since the observed levels are depopulating with relatively short lifetimes themselves. It can be demonstrated, however, that detailed information on the population dynamics and pathways can be derived once an appropriate model has been constructed. Figure 6 examines the build-up of the 985 nm emission shown in Figure 5. The form of the curve suggests the presence of several routes by which the $^4I_{11/2}$ level is excited in the upconversion process. We note that the time dependence observed for each of the other emitting levels is different and also complex. Differences are also apparent between host crystals. The complexity of a complete modeling suggests that the effort should await the identification of the most promising potential laser candidates before it is undertaken for a specific system.

Emission studies were made of the time dependence of the 1.54 μm emission from the $^4I_{13/2}$ level being excited by the short pulse Raman source. To avoid saturating the InSb detector by scattered pump light, a chopper operated in synchronism with the 1.54 μm pulse was employed to obscure the sample for the first 4 to 5 ms after excitation, and the decay recorded to beyond 50 ms. If we assume cooperative energy transfer among two $^4I_{13/2}$ erbium ions is responsible for the initial stages of the upconversion process, we can describe the $^4I_{13/2}$ population as

$$\frac{dN}{dt} = \frac{-N}{\tau_R} - 2wN^2 \qquad (1)$$

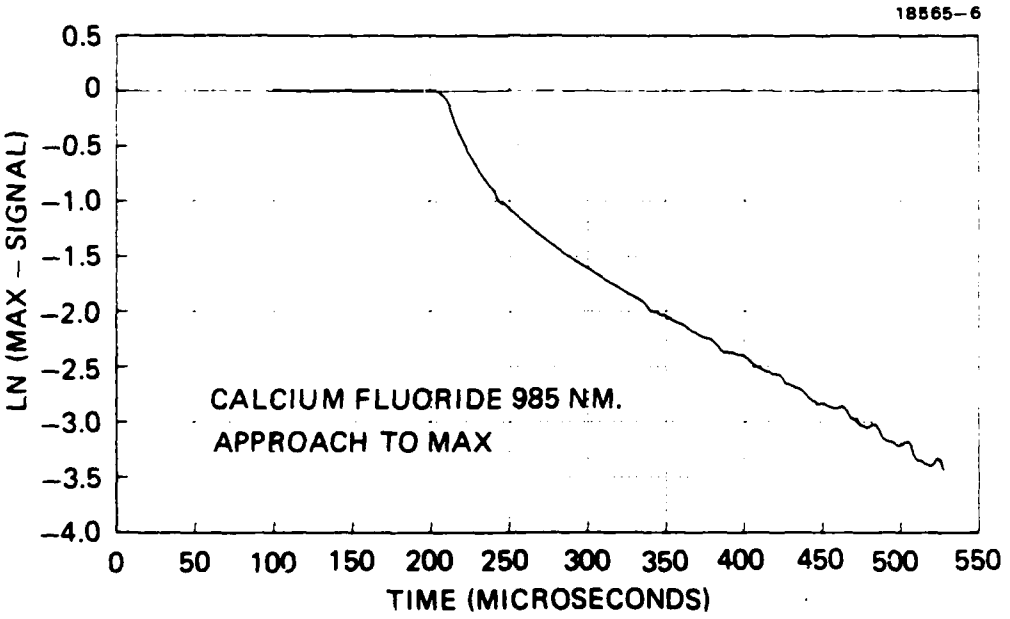

FIGURE 6. Early time approach to maximum population of $^4I_{11/2}$ level.

where τ_R is the radiative lifetime and w is the probability for cooperative energy transfer. The solutions of (1) can be written[3]

$$N(t) = \frac{N(0)}{[(1+\alpha)e^{t/\tau_R} - \alpha]} \qquad (2)$$

where $\alpha = 2w\tau_R N(0)$. In the present experiments we have not attempted to determine the initial $^4I_{13/2}$ population provided by the 1.54 μm pump pulse, and consequently are not yet able to determine the probability w. Nevertheless, our measurements show the expected nonexponential decay predicted by (2) and confirm the cooperative energy transfer mechanism. Of the several crystal and glass hosts measured, we found the 1.54 μm measurements on BaY_2F_8:Er 5% to exhibit this process most convincingly. Figure 7 displays the observed decay for this material. The scope trace initiated approximately 5 ms before the 10 ns, 1.54 μm excitation, and there was an additional 5 ms delay before the chopper blade exposed the sample. The finite risetime of the signal is related to the transit of the blade in the detection path.

The measurement data in Figure 7 were employed in a least squares fitting procedure to Eq. (2), from which the radiative lifetime of the $^4I_{13/2}$ level was determined.

Table 2. BaY_2F_8:Er 5% Lifetime

Level	1.54 μm Excitation	0.355 μm Excitation
$^4I_{13/2}$	15.8$\pm$1.0 ms	16.6$\pm$0.3 ms

The measurement (Table 2) is in good agreement with results discussed below using UV excitation to provide very clean single exponential decay. The curve marked "Pair Theory" in Figure 7 is a plot of Eq. (2) using the parameters derived from the fit.

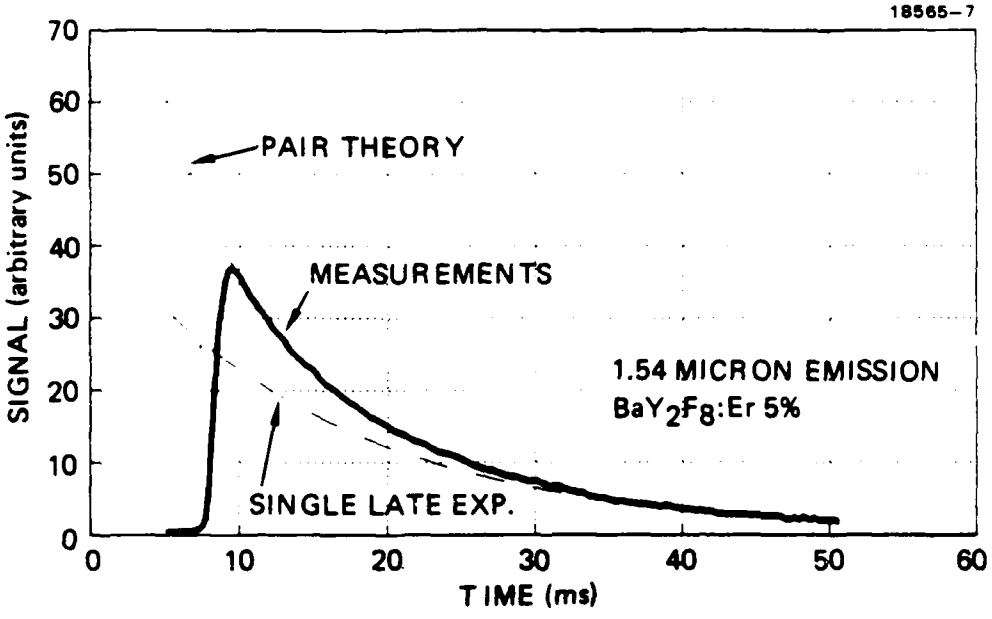

FIGURE 7. 1.54 μm emission from BaY_2F_8:Er 5%. The pair theory of Eq. (2) describes the measurements well. The dashed curve is the component due to radiative decay alone.

Also shown is the form of the decay curve computed using only the late-time exponential component. It is important to observe that cooperative energy processes are responsible for 50% of the population loss of the $^4I_{13/2}$ level in this experiment, and confirm important upconversion laser potential for BaY_2F_8:Er 5%. A logarithmic display is shown in Figure 8.

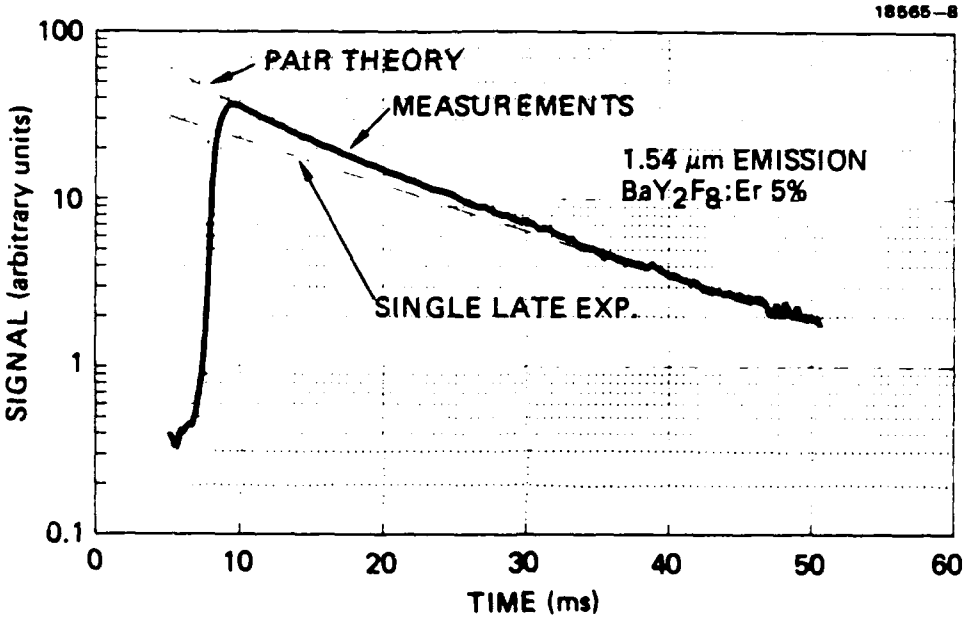

FIGURE 8. 1.54 μm emission from BaY_2F_8:Er 5%. The data are the same as in Figure 7.

SECTION 3

LASER EXPERIMENTS

3.1 PULSED PUMP EXCITATION - 1.54 μm

Three classes of experiments were carried out in an effort to obtain laser action at a number of wavelengths between 0.5 and 1.0 μm using erbium-doped hosts of CaF_2 and $YLiF_4$.

(1) Using 5 mm diameter rods of 1-in.-long crystals of CaF_2:Er 5% and $YLiF_4$:Er 5% cooled to 15K, we set up an optical cavity external to the dewar containing the crystal and employed mirrors for operation in turn at 551, 671, and 985 nm. These crystals were pumped through the cavity rear mirror by the 10 ns, 40 mJ, 1.54 μm pulses from the Raman-shifted source described above. No laser action was obtained in these experiments, although the upconversion mechanism did result in significant spontaneous emission at these wavelengths.

Two shortcomings of this experiment can be identified. The vacuum windows in the low-temperature optical dewar and the plane ends of the laser rod were not provided with dielectric antireflection coatings, and contributed therefore a single-pass optical loss that exceeded 20%. Successful laser operation thus required a population inversion on the respective transitions capable of providing gain in excess of this value.

Further, it became apparent during these experiments that the longitudinal extent of the pumped region, as indicated by the length over which upconverted emission was visible, was <1 cm. As this was not the case in the 2.7 μm laser experiments reported in the second annual report on this contract, very detailed absorption data were measured on the materials under study and are summarized in Appendix A. Under conditions of the 40 mJ pump source, we estimated that an active length no longer than 5 mm would be appropriate to avoid substantial unpumped regions along the length of the rod.

(2) As noted above, the previous annual report discussed the successful operation of a 2.7 μm laser on the $^4I_{11/2} \rightarrow {}^4I_{13/2}$ transition in $YLiF_4$:Er 5%. The laser rod in this experiment was 75 mm long and was pumped by a 200-mJ-long-pulse (~1 ms) erbium-doped phosphate glass laser operating at 1.53 μm. Transmission measurements through the $YLiF_4$ rod demonstrated that saturation of the $^4I_{15/2} \rightarrow {}^4I_{13/2}$ 1.53 μm pump transition allowed the longer length of laser rod to be used. The operative excitation mechanism exploits the cooperative energy exchange between $^4I_{13/2}$ ion pairs to produce a ground-state ion and a $^4I_{9/2}$ ion. Rapid nonradiative decay out of the $^4I_{9/2}$ level provides population in the $^4I_{11/2}$ upper laser level.

It should be possible to employ this same mechanism to obtain 985 nm laser action in this system on the $^4I_{11/2} \rightarrow {}^4I_{15/2}$ transition if the system is adequately cooled to depopulate the upper Stark split components of the $^4I_{15/2}$ ground state. S.A. Pollack of the Hughes Aircraft Support Systems Group, where the 2.7 μm laser study was carried out, repeated the experiment, replacing the 2.7 μm laser mirrors with 985 nm mirrors. No 985 nm laser operation was achieved. Pollack carried out important subsequent experiments on a related IR&D project and was able to demonstrate excitation of the $^4S_{3/2}$ level of erbium in $YLiF_4$ by a three-fold upconversion process. With pumping at 1.53 μm, laser operation was achieved on the following transitions:

$^4S_{3/2} \rightarrow {}^4I_{9/2}$	1.73 μm
$^4S_{3/2} \rightarrow {}^4I_{11/2}$	1.23 μm
$^4S_{3/2} \rightarrow {}^4I_{13/2}$	0.85 μm .

Experiments intended to demonstrate laser operation on the $^4S_{3/2} \rightarrow {}^4I_{15/2}$ transition at 551 nm have not been successful under 1.53 μm pumping in this system. Experiments reported by L.F. Johnson and H.J. Guggenheim[5] using a series of BaY_2F_8:Er crystals suggest that the system can experience substantial loss

at 551 nm resulting from absorption at this wavelength on the $^4I_{13/2} \rightarrow {}^2H_{9/2}$ transition. We will see below that absorption on this transition appears to result in Q-switched operation at 551 nm when an alternative $^4S_{3/2}$ excitation pathway is successfully obtained.

(3) To further explore the use of the higher repetition rate 1.54 μm Raman-shifted 10 ns, 40 mJ pump source, we fabricated shorter laser rods from CaF_2:Er 5%, $YLiF_4$:Er 5%, and ZBLAN:Er 4% materials. Cavities were made 5 mm in length with 3-cm-radius spherical convex surfaces on which dielectric mirrors were deposited. With particular attention to 551 and 671 nm laser operation, we specified one mirror to be high reflectivity at these wavelengths and provide 85% transmission at 1.5 μm. This coating also provided good transmission at 791 nm. The mirror to be employed for laser output coupling provided 0.5% transmission at 551 and 671 nm, rising significantly and rapidly outside these limits, particularly in the green. The damage limit specified for the dielectric coatings was 250 MW/cm^2, requiring that the 10 ns, 40 mJ pump pulse be focused no more tightly than 1.4 mm in diameter. The diameter of the TEM_{00} mode in the crystal cavities was computed to be between 60 and 70 μm, depending on the wavelength, and therefore a serious inefficiency in pump energy utilization occurred.

The first laser experiments were carried out using the $YLiF_4$:Er 5% crystal, as suggested by the observations of Pollack discussed above. No laser emission was observed over the entire temperature range from 15K to room temperature, even though strong spontaneous emission occurred at the wavelengths of interest, 551 and 671 nm. Coatings for 985 nm were not prepared.

The peak intensity of the spontaneous emission at 551 and 671 nm was found to depend on temperature. The normalized peak data for each wavelength are shown in Figure 9. It remains to be established whether the result is due to a temperature-

dependent shift of the particular Stark split component of the $^4I_{15/2} \rightarrow {}^4I_{13/2}$ transition being pumped by the Raman source, or due to lifetime changes with temperature of the energy levels responsible for the upconversion process. Indeed the $^4S_{3/2}$ data used for Figure 9 show an increase in decay lifetime with decreasing temperature (necessarily associated with the level responsible for upconversion), as well as changes in the shape of the time dependence, which suggests changes in the pump path complexity as well. The lifetime history data for the 671 nm $^4F_{9/2}$ level remain to be analyzed.

3.2 CW PUMP EXCITATION - 791 nm

Using cw excitation provided by a Coherent Model 699 dye laser operating at 791 nm, we achieved upconversion laser operation using the 5 mm $YLiF_4$:Er 5% laser rod described above. The transitions observed were

$^4F_{9/2} \rightarrow {}^4I_{15/2}$	671 nm
$^4S_{3/2} \rightarrow {}^4I_{15/2}$	551 nm .

As supplied by the optical fabrication and coating vendor, the laser operated only at 671 nm in our initial experiments. The laser output was strictly cw and the system operated up to 60K. By incorporating an additional external spherical mirror at the output side of the dewar holding the crystal, in order to provide an increased reflectivity at 551 nm, we obtained laser oscillation in a pulsed mode at this second wavelength. This laser transition in $YLiF_4$ has been reported by IBM workers,[6] who employed cw pumping on a different Stark split component of $^4I_{15/2} \rightarrow {}^4I_{9/2}$ at 8020 Å. Figure 10 shows the train of ~100 ns pulses. The repetition frequency was ~100 kHz and was found to increase as the pump excitation level was increased. As noted earlier, L.F. Johnson and H.J. Guggenheim[5] ascribe Q-switched operation to saturable losses on a resonant transition $^4I_{13/2} \rightarrow {}^2H_{9/2}$, which overlaps the wavelength of the laser at

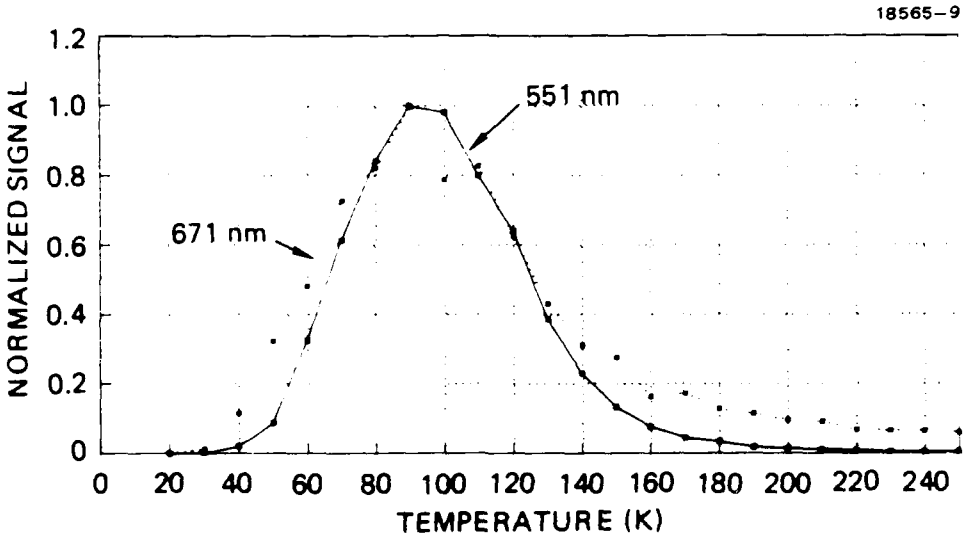

FIGURE 9. Temperature dependence of fluorescence from $YLiF_4$:Er 5% from the $^4S_{3/2}$ and $^4F_{9/2}$ levels for 1.54 μm excitation.

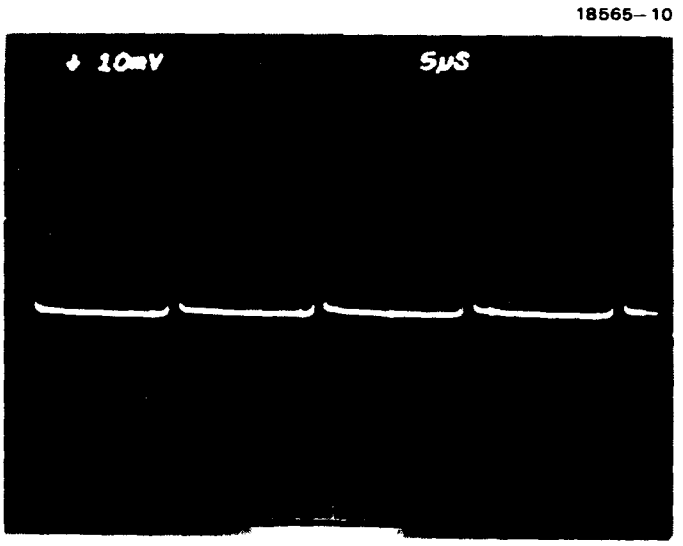

FIGURE 10. 551-nm output pulse train.

551 nm. Laser operation at 551 nm persisted up to 85K. Later experiments with better pump alignment produced 2.5 mW average output power without the external mirror noted above. Optimum temperature was 65K.

The cw transition at 671 nm has not previously been reported for $YLiF_4$:Er 5%. Flashlamp pumping of BaY_2F_8:Er by Johnson and Guggenheim[5] achieved pulsed operation at this and other wavelengths. To establish the details of the excitation pathway of the $^4F_{9/2}$ upper lased level for the cw system, we observed the build-up of laser oscillation as the 791 nm pump was turned on using a high speed (5 ns) Pockels cell shutter. As shown in Figure 11, a delay of 0.6 ms was observed for 260 mW pump power before laser action commenced. This extended to approximately 1.2 ms when the pump power was reduced to 140 mW. Of particular interest was the appearance of two components in the approach of the laser to steady state, which suggests two pumping pathways. One has an approximately 0.5 ms risetime, which is suggestive of a radiative lifetime, and is followed by a slower component that appears to be several milliseconds long and could be excitation dependent. More measurements are required to determine the details of these processes.

Candidate pumping pathways involve energy sharing by cooperative processes of $^4I_{11/2}$ ion pairs to populate ^2G or ^2H levels above 20,000 cm^{-1}, from which spontaneous emission or phonon processes populate the $^4S_{3/2}$ and $^4F_{9/2}$ upper laser levels. A second excitation pathway involves an alternative sequential zigzag absorption process:

$$^4I_{15/2} + h\nu \rightarrow {}^4I_{9/2}$$
$$^4I_{9/2} \rightarrow {}^4I_{13/2} + \text{phonons or spontaneous emission}$$

$$^4I_{13/2} + h\nu \rightarrow {}^2H_{11/2}$$
$$^2H_{11/2} \rightarrow {}^4S_{3/2} \text{ or } {}^4F_{9/2} + \text{phonons or spontaneous emission}$$

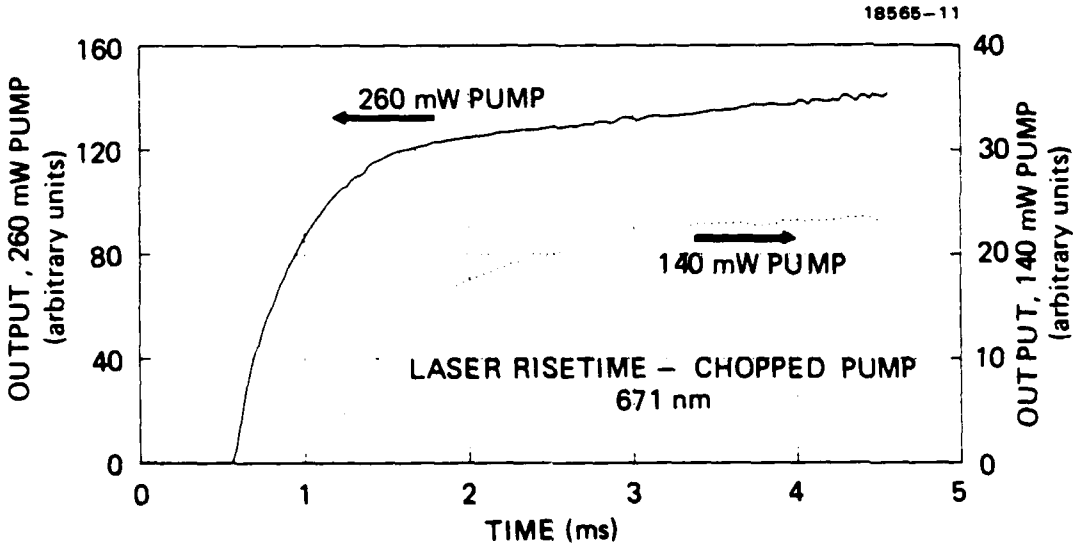

FIGURE 11. Build-up of cw laser output at 671 nm. Pump starts at t = 0.

Evidence that this two-step absorption of pump photons is operative follows from the observation that laser oscillation at 671 nm is not cw when laser emission occurs simultaneously at 551 nm. The Q-switched behavior of the $^4S_{3/2} \rightarrow {}^4I_{15/2}$ transition arises from saturation of the transition $^4I_{13/2} \rightarrow {}^2H_{9/2}$, which imparts a time dependence to the $^4I_{13/2}$ population. This then modulates the second pumping step in the above pumping chain for $^4F_{9/2}$ production. Figure 12 displays the time dependence imparted to the 671 nm laser output when the 551 nm operation is allowed to take place. It would be expected that an explicit relationship would be found between the periodicity observed at each of the simultaneously oscillating wavelengths. While this relationship has been observed to be the case on several occasions, it has been experimentally difficult to demonstrate unequivocally. The period measured at 671 nm in Figure 11 is less than that that would be imposed by Q-switching at the 551 nm wavelength. While no high resolution spectral analysis has been carried out, the multiple Stark split levels could contribute to several laser output wavelength components and substantially complicate the transient dynamics of the populations of the participating energy levels.

The variation in cw laser output power at 671 nm with input pump power at 791 nm is shown in Figure 13. The data were taken over a pump range from 127 to 285 mW and it is estimated that the pump threshold is approximately 80 mW. The curve is consistent with a two-fold upconversion process but shows a saturation at high pump powers. Using the 0.5% output coupling, we have obtained 1 mW cw output at 300 mW pump input. The optimum temperature is approximately 50K and the laser changes from red to green operation exclusively as the temperature is raised to 65K.

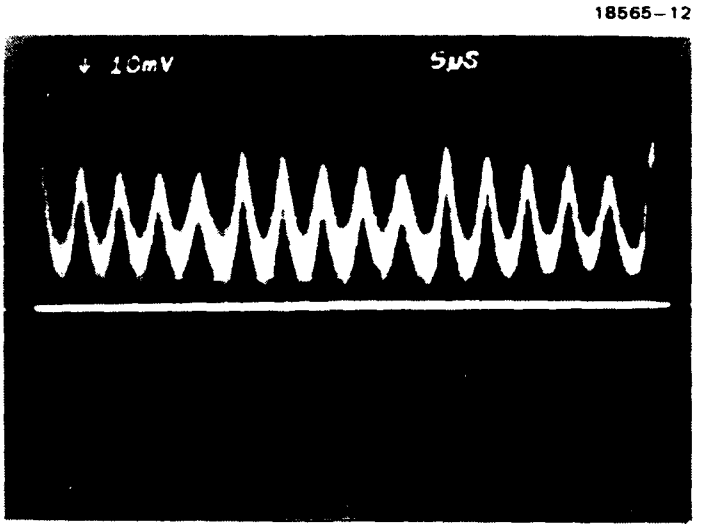

FIGURE 12. 671-nm output modulation occurring when 551 nm transition is simultaneously present.

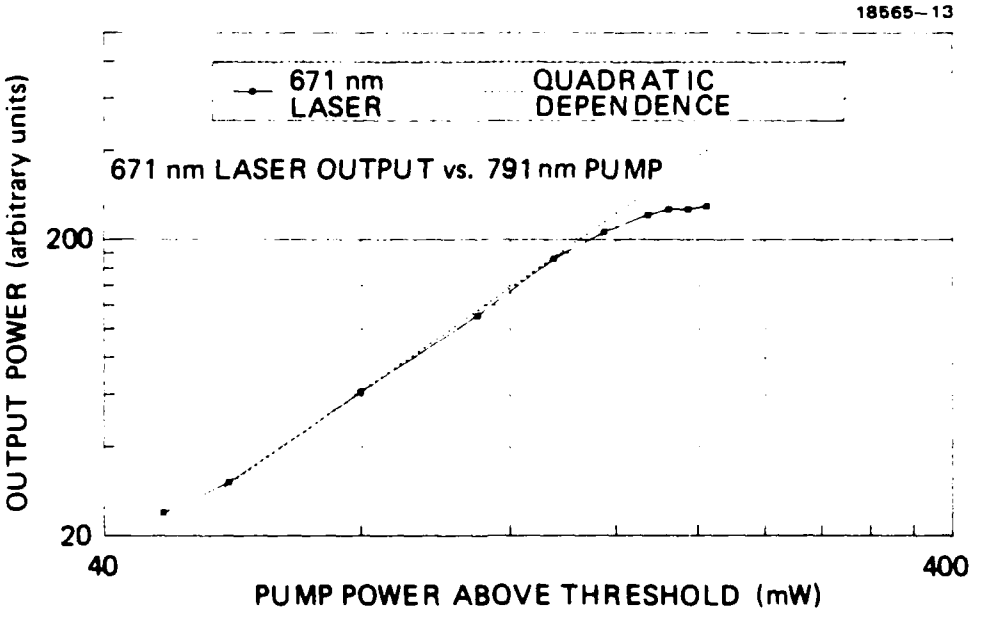

FIGURE 13. Variation of 671 nm laser output with pump power above threshold.

SECTION 4

NEW MATERIALS AND DIRECTIONS

During the final year of this program, detailed data were acquired on the absorption spectra of the several laser materials under study. The results are summarized in Appendix A for CaF_2:Er 5%, $YLiF_4$:Er 5%, and ZBLAN:Er 4%. Included are expanded displays for the 1.54 μm and 800 nm pump bands to permit a determination of crystal sizes for optimum pumping conditions. To date our cw pumping experiments have been successful only with the $YLiF_4$:Er 5% system. This material has the narrowest linewidth spectral features of the three systems examined. All are attractive candidates for pumping by laser diodes, not only for visible upconversion operation, but also for laser operation at 2.7 μm. The ZBLAN is particularly attractive for this mid-IR operation, as it is estimated to be ultimately capable of providing fibers of substantially lower loss than those of silica.

Initial work supported by IR&D funding has been completed in collaboration with M. Robinson of HRL on the preparation and measurements of other erbium-doped crystal systems that exhibit narrow line spectral features and, where possible, contain substantially higher erbium concentrations. As discussed above, the crystal BaY_2F_8:Er 5% in our first experiments showed under excitation at 1.54 μm that pair processes were responsible for 50% of the energy disposal out of the $^4I_{13/2}$ level. The population density of the $^4I_{13/2}$ initially excited remains to be determined.

The extinction coefficient for BaY_2F_8:Er 5% measured on a Perkin-Elmer Lambda 9 instrument is shown in Figure 14, and the details of the structure at 800 nm are shown in Figure 15. The system appears at least as well resolved as the features measured for $YLiF_4$:Er 5%. The structure at 1.5 μm, shown in

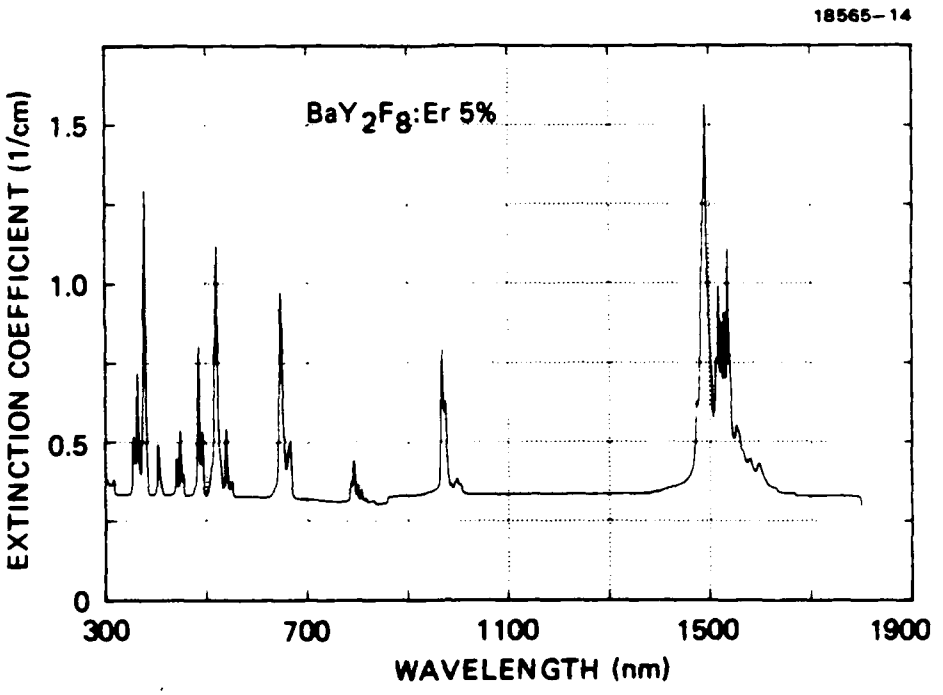

FIGURE 14. Extinction coefficient for BaY_2F_8:Er 5%.

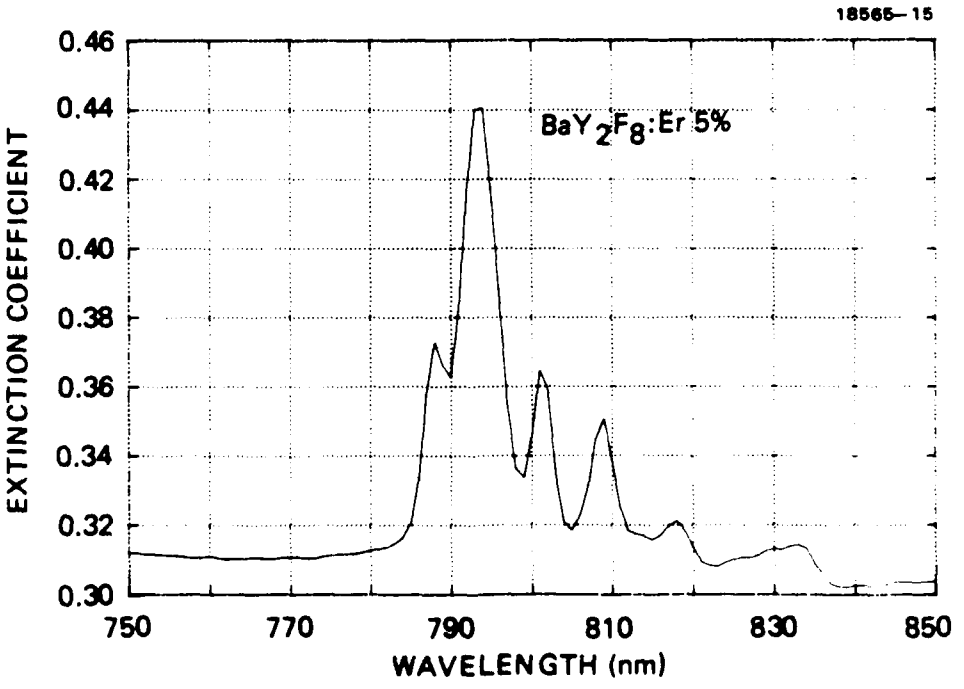

FIGURE 15. Extinction coefficient for BaY_2F_8:Er 5% at the $^4I_{15/2} \rightarrow {}^4I_{9/2}$ pump band.

Figure 16, reveals the details of the $^4I_{15/2} \rightarrow {}^4I_{13/2}$ transition. The system merits examination as a candidate for diode laser excitation.

To further examine the BaY_2F_8:Er 5% system, we have begun a study of the lifetimes of the energy levels of importance for both visible and mid-IR laser application. To avoid the complexity of pair process modeling discussed earlier, we excited small crystal samples with a 10 ns pulse at 355 nm, derived by frequency tripling the 1.06 μm Nd:YAG laser. Simple single exponential decays were measured for the $^4I_{13/2}$ and $^4I_{11/2}$ levels. The observed signals are shown in Figures 17 through 20, with both linear and logarithmic presentations.

Lifetimes for the two levels are shown in Table 3. The measurement for $^4I_{13/2}$ is in good agreement with the value inferred from the pair model under 1.54 μm excitation. Data have been acquired on the $^4S_{3/2}$, $^4F_{9/2}$, and $^4I_{9/2}$ levels for BaY_2F_8:Er 5% but have not been analyzed.

Initial spectral measurements have been made on crystals having much higher erbium densities. Figure 21 shows the absorption spectrum of $YErLiF_4$, where 50% of the yttrium has been replaced by erbium. The extinction coefficients are very large and the expanded presentation in Figure 22 shows the spectral structure near 800 nm continues to be well-resolved. This particular sample contained 0.5% holmium, which is

Table 3. Lifetimes BaY_2F_8:Er 5%.

Level	Lifetimes
$^4I_{11/2}$	10.4 ± 0.2 ms
$^4I_{13/2}$	16.6 ± 0.3 ms

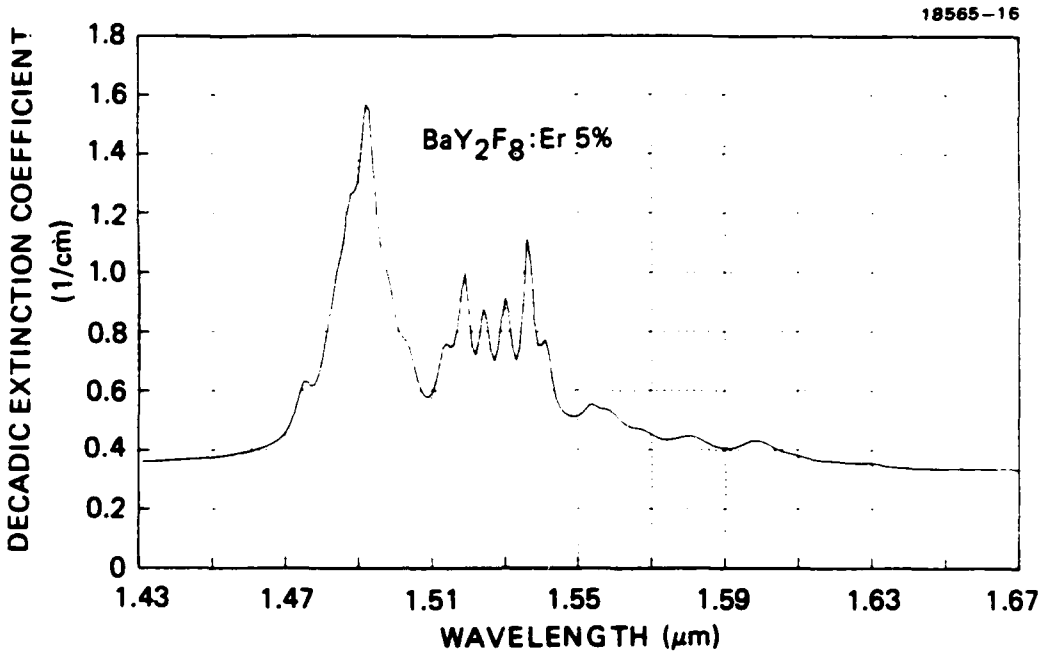

FIGURE 16. Extinction coefficient for BaY_2F_8:Er 5% at the $^4I_{15/2} \rightarrow {}^4I_{13/2}$ pump band.

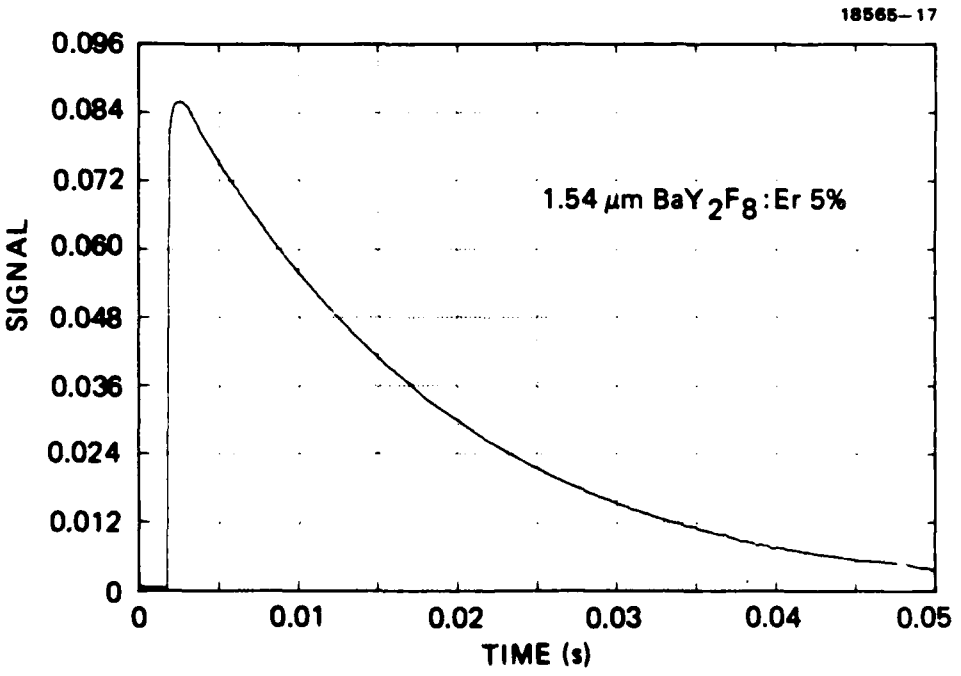

FIGURE 17. Decay of $^4I_{13/2}$ in BaY_2F_8:Er 5% under short pulse UV excitation.

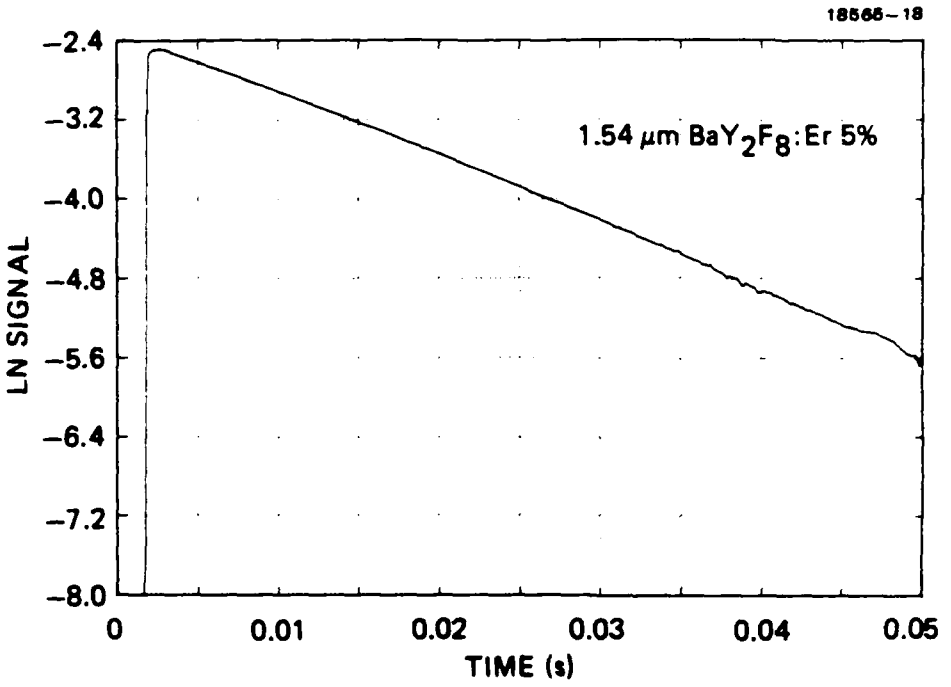

FIGURE 18. Logarithmic decay of $^4I_{13/2}$ in BaY_2F_8:Er 5% under short pulse UV excitation.

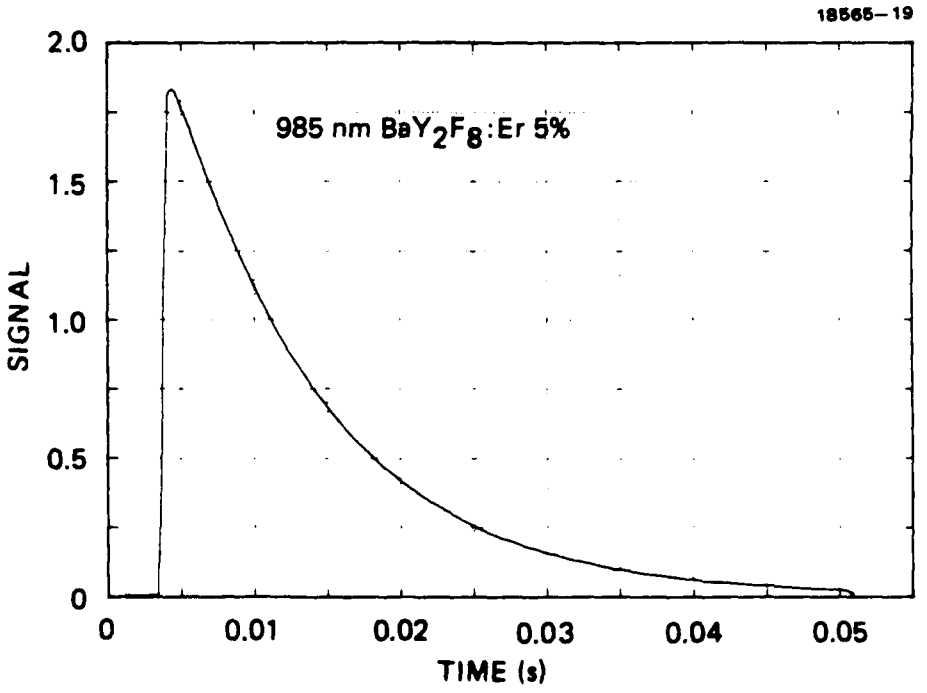

FIGURE 19. Decay of $^4I_{11/2}$ in BaY_2F_8:Er 5% under short pulse UV excitation.

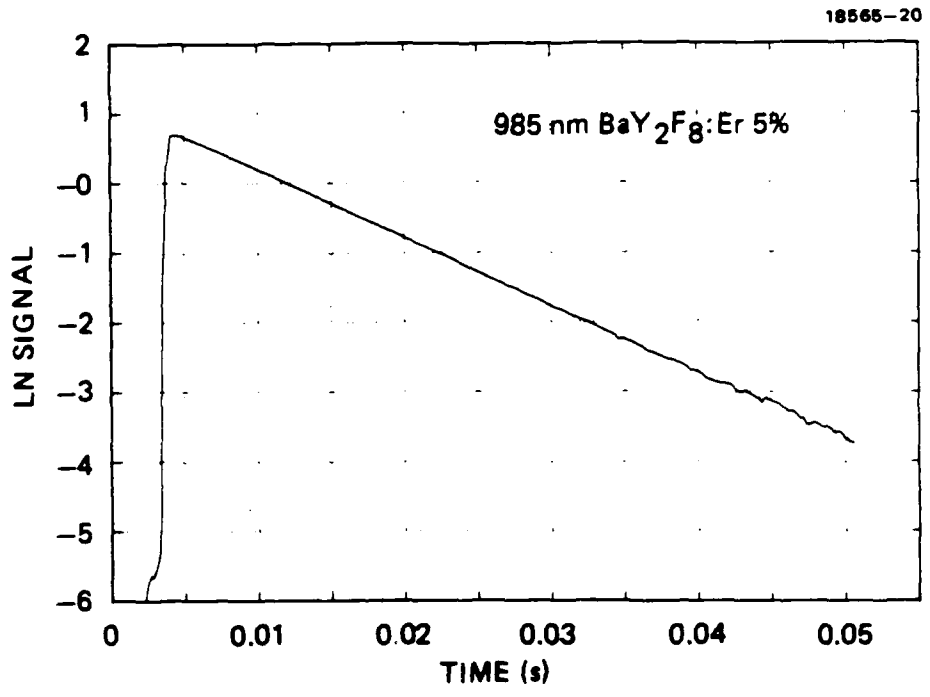

FIGURE 20. Logarithmic decay of $^4I_{11/2}$ in BaY_2F_8:Er 5% under short pulse UV excitation.

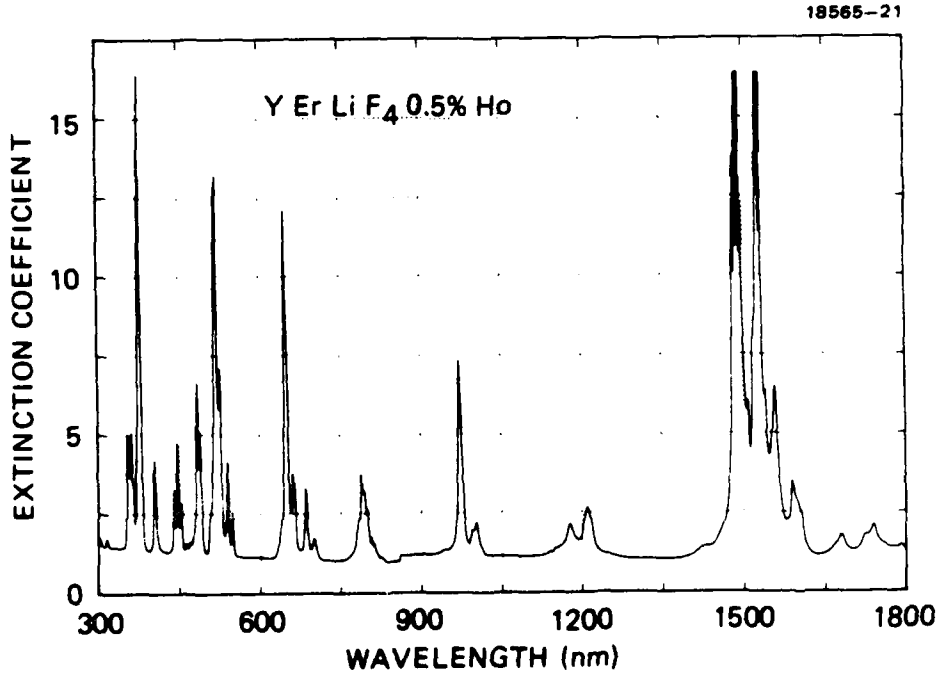

FIGURE 21. Extinction coefficient for $YErLiF_4$:Ho 0.5%.

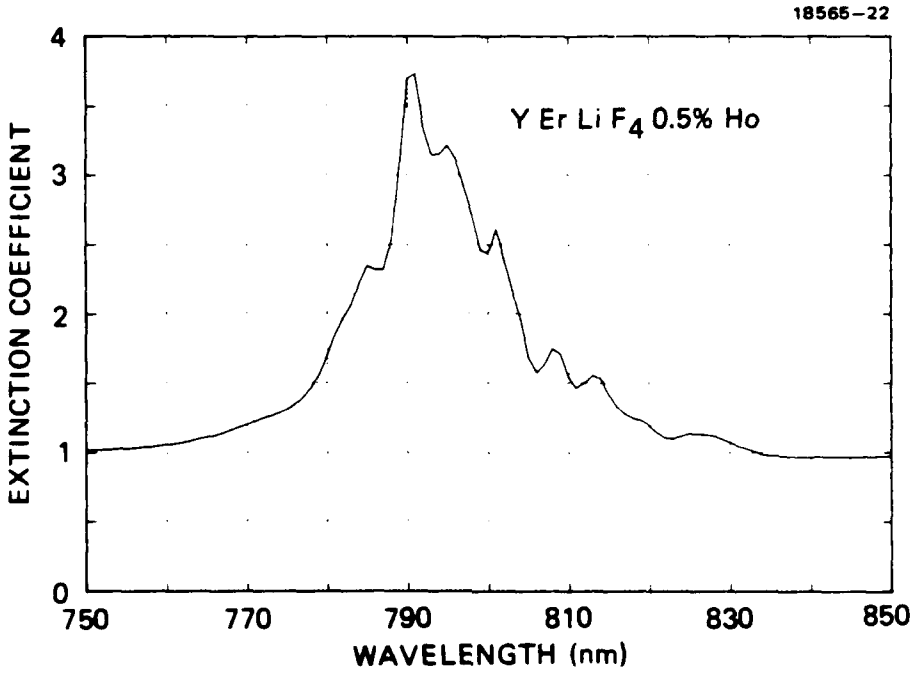

FIGURE 22. Extinction coefficient for $YErLiF_4$:Ho 0.5% at the $^4I_{15/2} \rightarrow {}^4I_{9/2}$ pump band.

responsible for the 1200 nm feature of Figure 21. Measurements in ErF_3 are shown in Figures 23 and 24. Again, spectral features are well-resolved.

These new materials require measurements of the electronic state lifetimes and optical cross-sections to provide the initial data for evaluating them as potential laser materials. Again, both upconversion operation and mid-IR laser (1.7 and 2.7 μm) potential using diode pumping are attractive. The very short optical path lengths (1 to 2 mm) required for complete pump absorption could provide extremely compact sources when diode pumped.

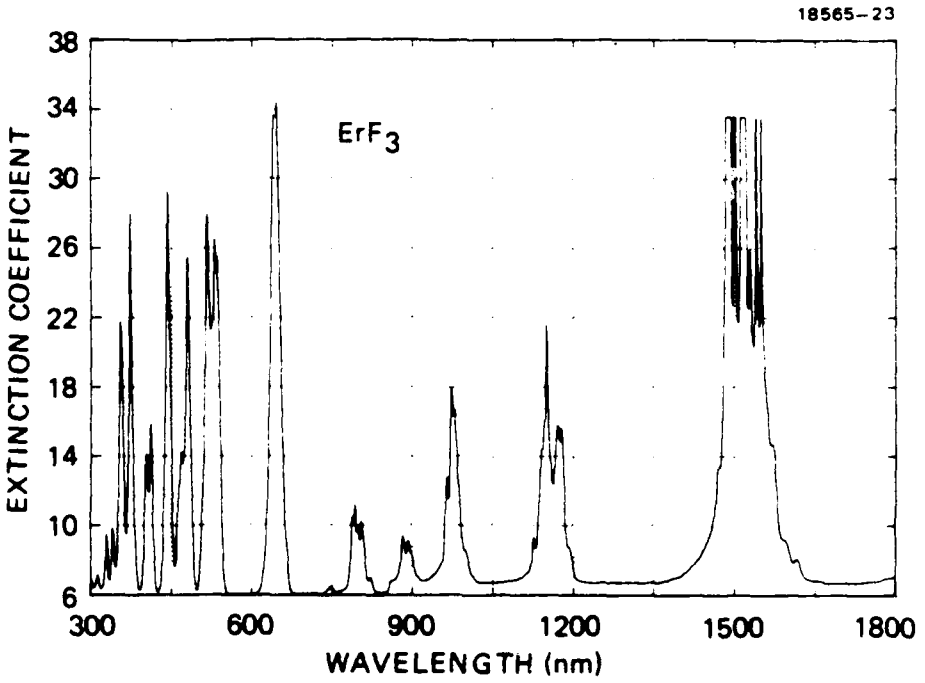

FIGURE 23. Extinction coefficient for ErF_3.

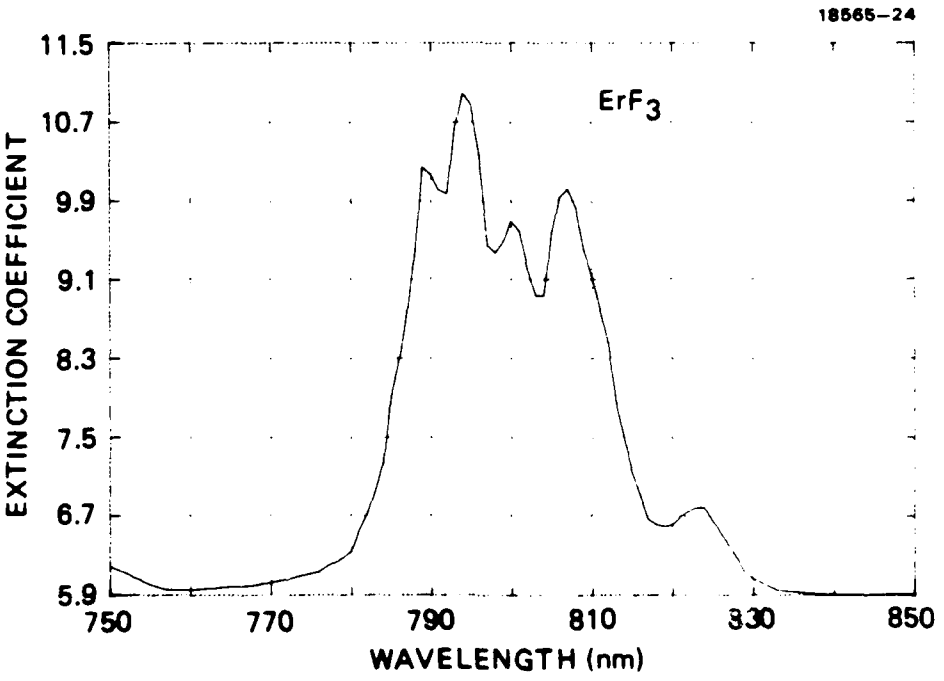

FIGURE 24. Extinction coefficient for ErF_3 at the $^4I_{15/2} \rightarrow {}^4I_{9/2}$ pump band.

APPENDIX A

The following pages (Figures 25 through 33) contain data on the extinction coefficient as a function of wavelength for:

CaF_2:Er 5%

$YLiF_4$:Er 5%

ZBLAN:Er 4%

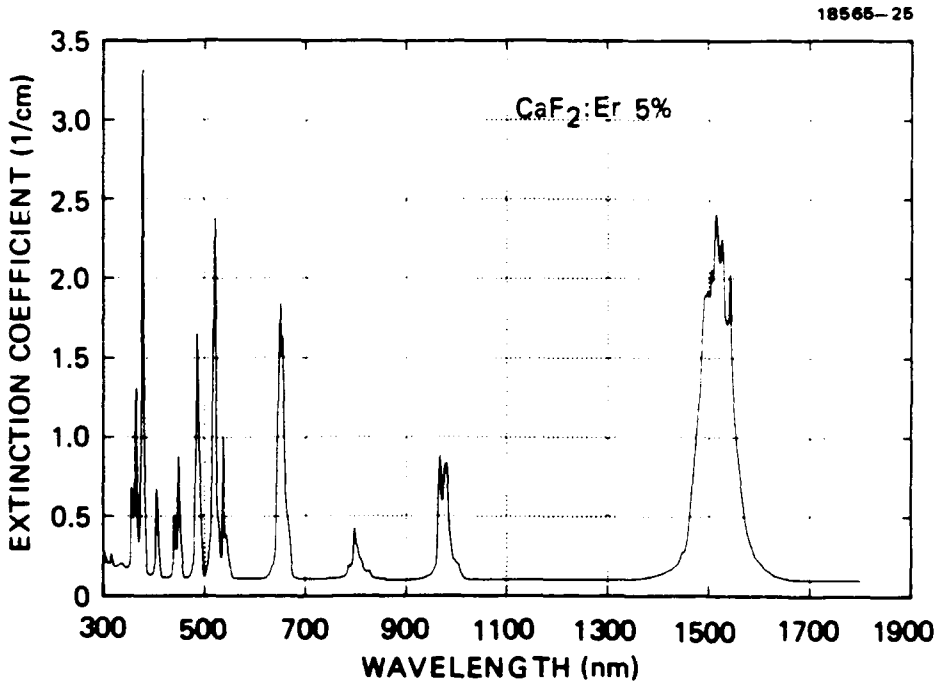

FIGURE 25. Extinction coefficient for CaF_2:Er 5%.

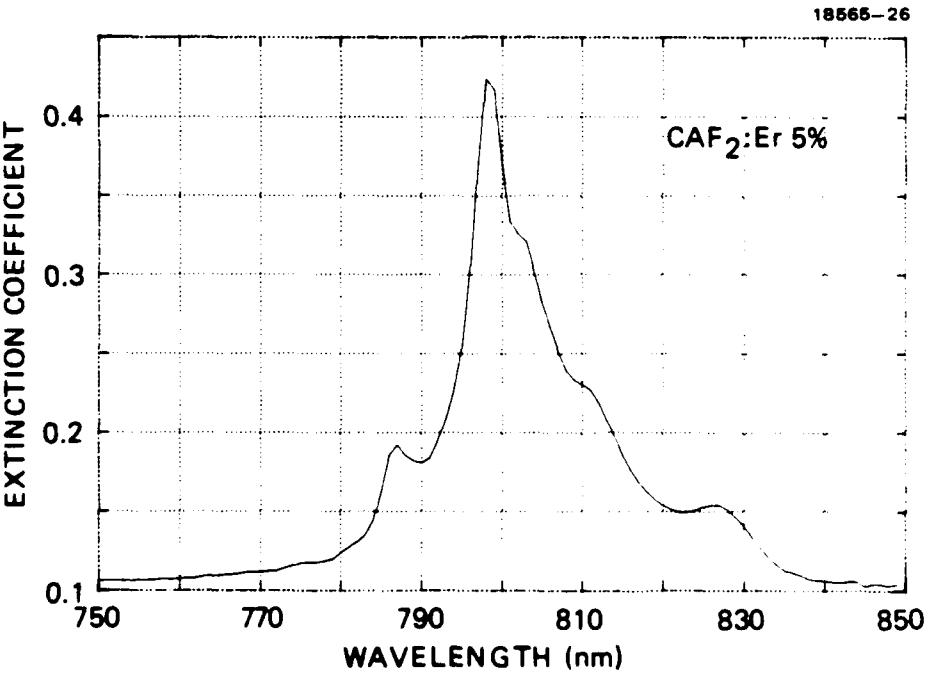

FIGURE 26. Extinction coefficient for CaF_2 at the $^4I_{15/2} \rightarrow {}^4I_{9/2}$ pump band.

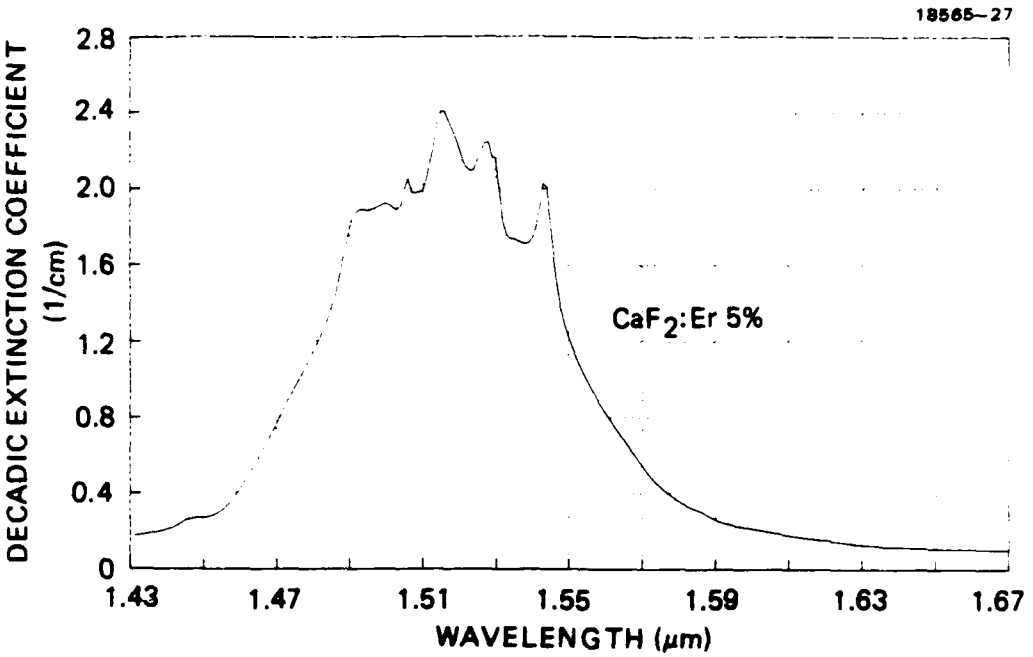

FIGURE 27. Extinction coefficient for CaF_2 at the $^4I_{15/2} \rightarrow {}^4I_{13/2}$ pump band.

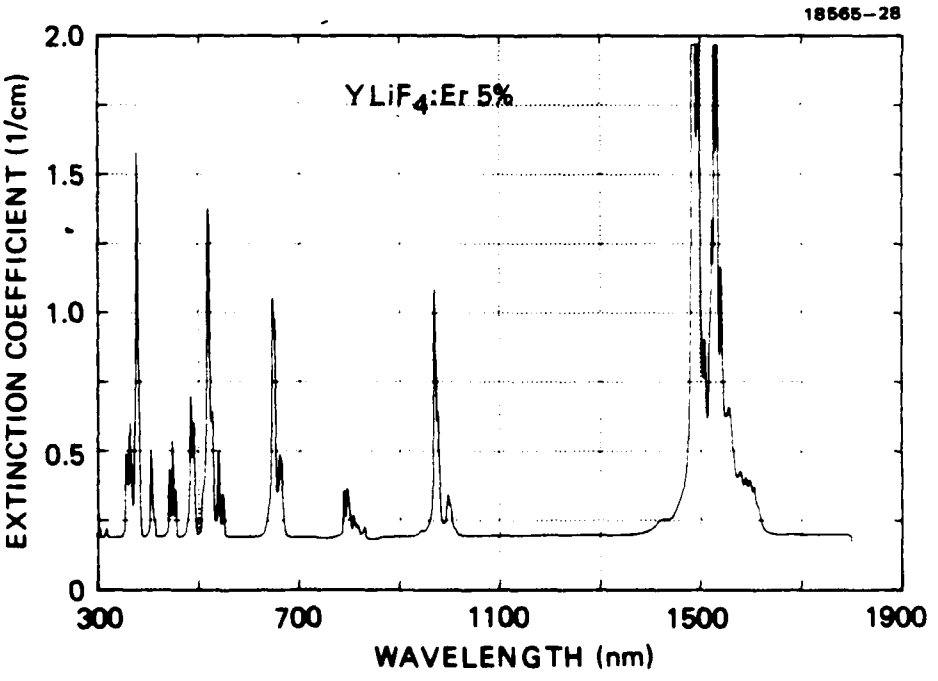

FIGURE 28. Extinction coefficient for $YLiF_4$:Er 5%.

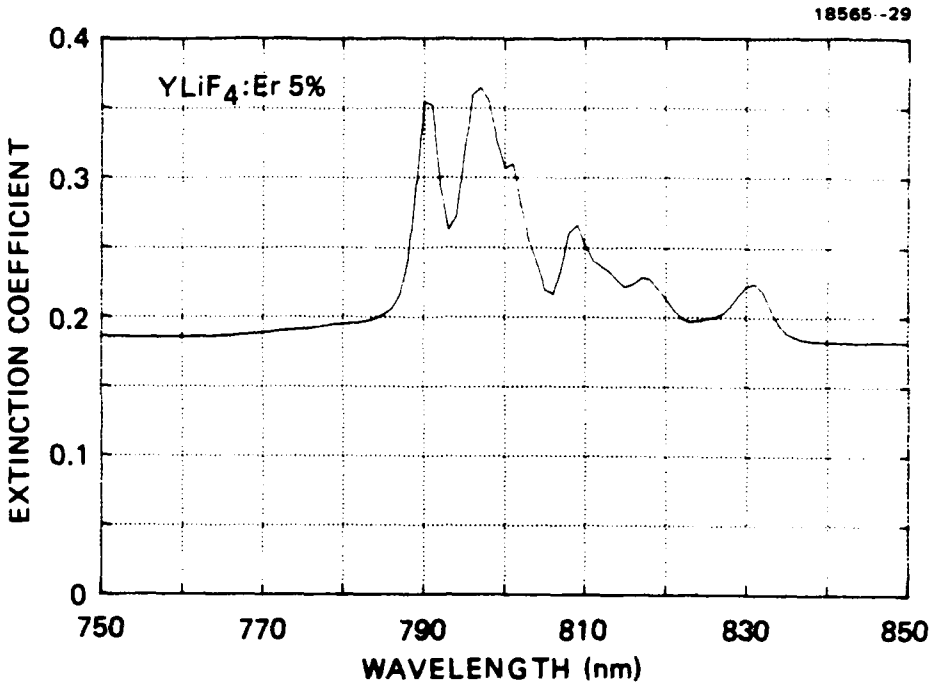

FIGURE 29. Extinction coefficient for $YLiF_4$:Er 5% at the $^4I_{15/2} \rightarrow {}^4I_{9/2}$ pump band.

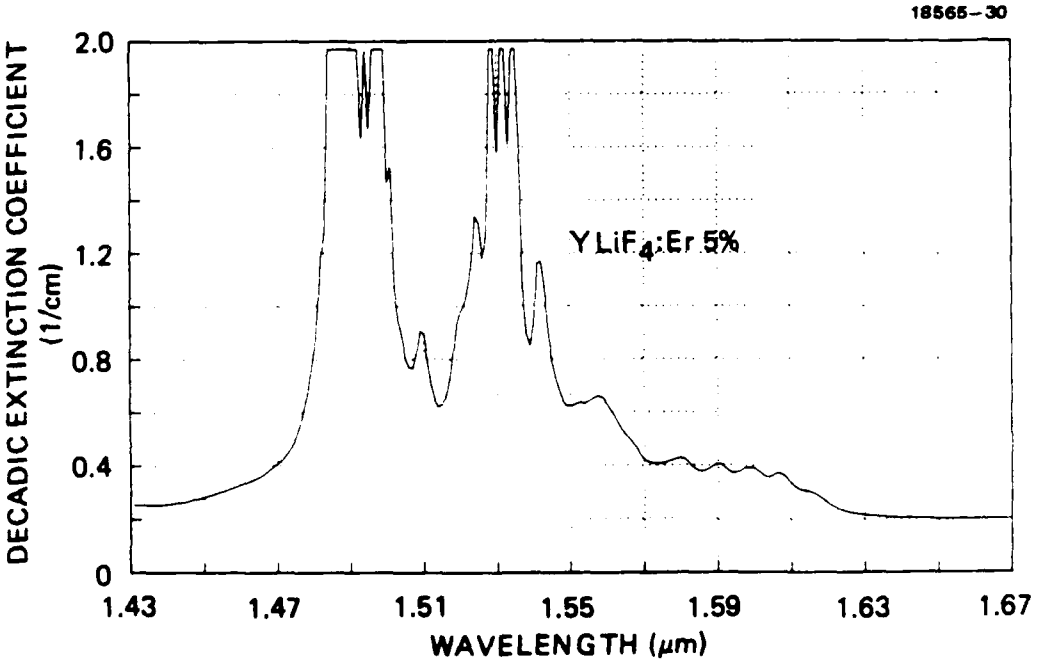

FIGURE 30. Extinction coefficient for $YLiF_4$:Er 5% at the $^4I_{15/2} \rightarrow {}^4I_{13/2}$ pump band.

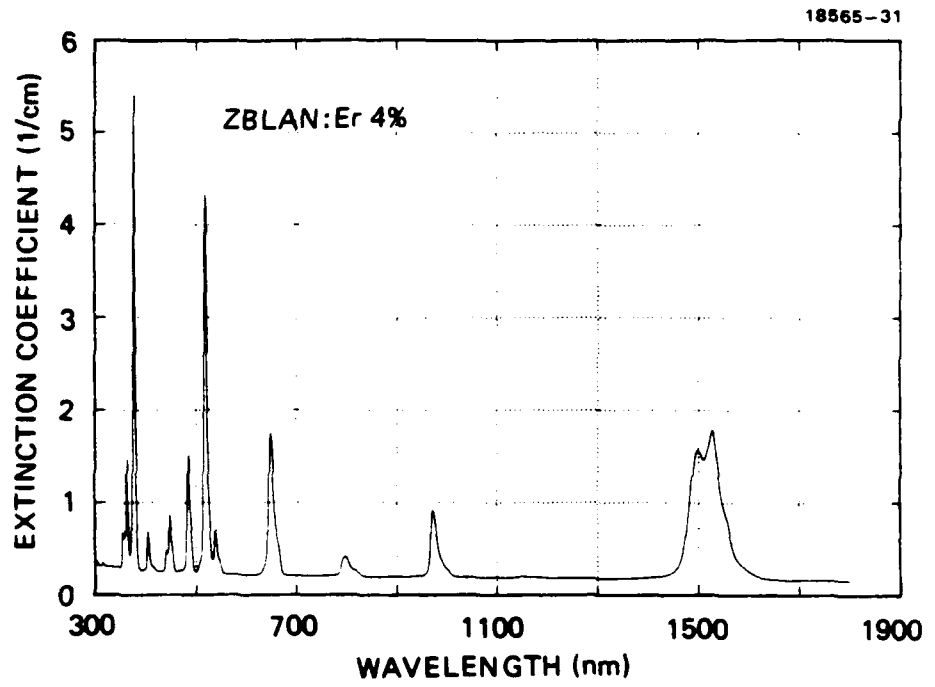

FIGURE 31. Extinction coefficient for ZBLAN:Er 4%.

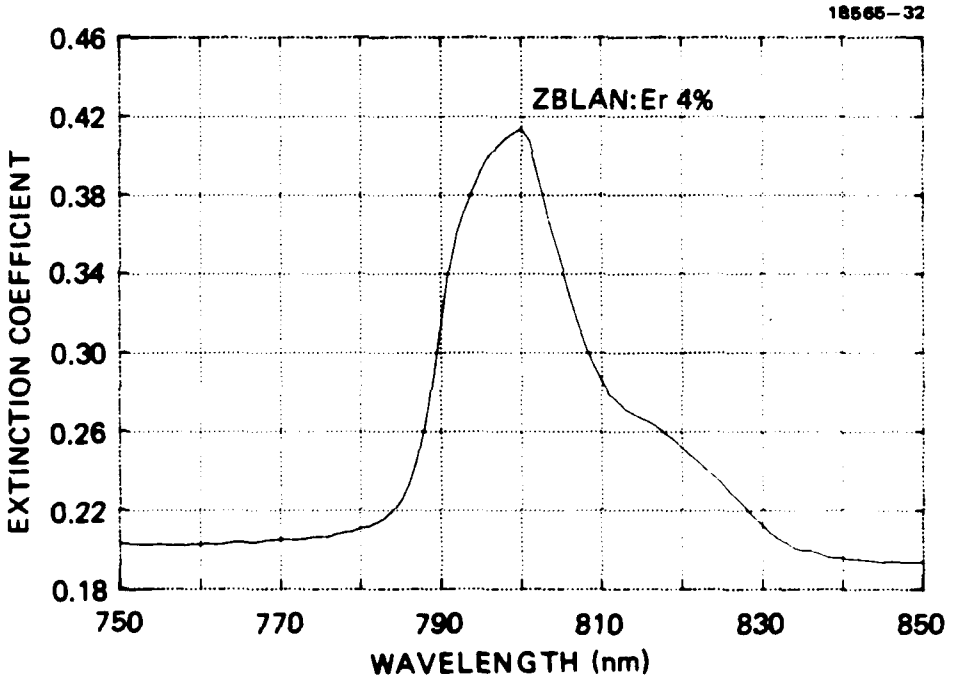

FIGURE 32. Extinction coefficient for ZBLAN:Er 4% at the $^4I_{15/2} \rightarrow {}^4I_{9/2}$ pump band.

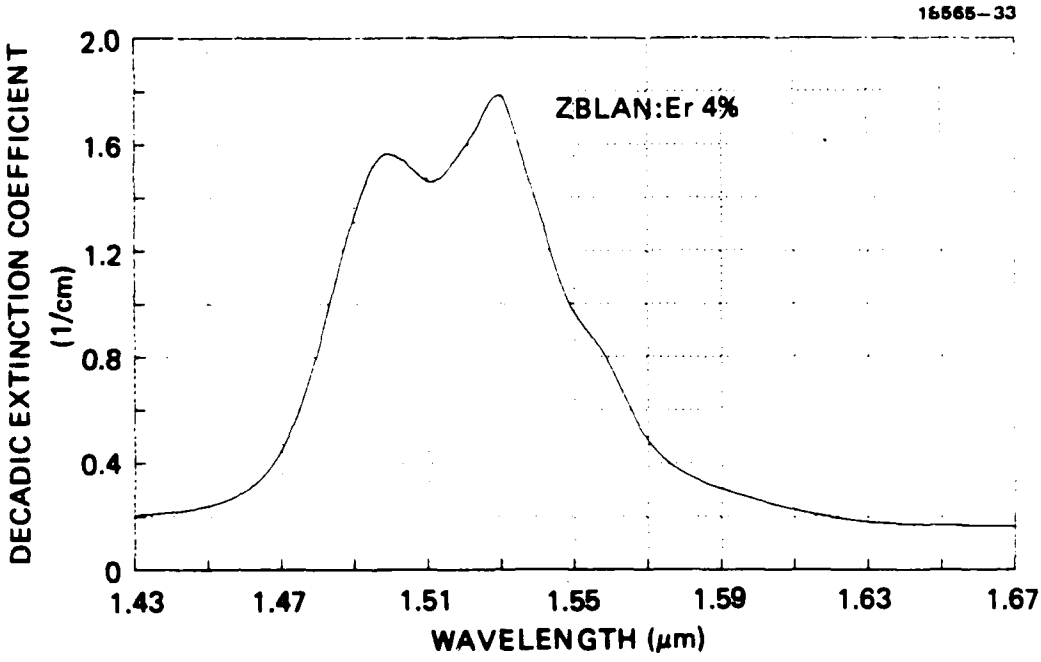

FIGURE 33. Extinction coefficient for ZBLAN:Er 4% at the $^4I_{15/2} \rightarrow {}^4I_{13/2}$ pump band.

PUBLICATIONS AND PRESENTATIONS

This section is a list of publications and presentations made during the contract period.

1. S.C. Rand (invited), "Continuous-wave Phase Conjugation with F-Aggregate Color Centers in LiF," Fifth International Conference on Dynamical Processes in the Excited States of Solids, July 1-4, 1985, Villeurbanne, France.

2. D.G. Steel, S.C. Rand, and J. Remillard, "Ultra-narrow Optical Resonances and Measurements of Relaxation Rates Using Resonant Four-Wave Mixing," International Quantum Electronics Conference, June 9-13, 1986, San Francisco.

3. S.C. Rand, "Intersystem Crossing of F_2 Color Centers Studied by Four-wave Mixing Spectroscopy," Optics Letters 11, 135 (1986).

4. S.C. Rand, "Continuous-wave Phase Conjugation with F-Aggregate Color Centers in LiF," Journal de Physique (France) 46, C7-507 (1985).

5. J.F. Lam and S.C. Rand, "Dressed atom theory of stimulated pair transitions," Phys. Rev. 35A, 2164 (1987).

6. J.F. Lam, S.C. Rand, and R.A. McFarlane, "Resonant optical suppression of the van der Waals force," presented at the Eighth International Conference on Laser Spectroscopy (EICOLS'87), Sweden, June 22-26, 1987.

7. S.C. Rand and S.A. Pollack, "Pair-pumped upconversion solid state laser," presented at the Annual Meeting of the Optical Society, Rochester, N.Y., October 1987.

8. S.C. Rand and S.A. Pollack, "Pair-pumped upconversion laser," presented at the Third International Laser Science Conference, November 1-5, 1987.

9. S.C. Rand "Four-wave mixing spectroscopy of metastable defect states in solids," in Lasers, Spectroscopy and Ideas-A Tribute to A.L. Schawlow, Springer-Verlag, Berlin, 1987.

10. S.C. Rand, J.F. Lam, R.S. Turley, R.A. McFarlane, and O.M. Stafsudd, "Optical pair interactions in the four-wave mixing spectrum of Nd:β"-Na-Alumina," Phys. Rev. Lett. 59, 597, 1987.

11. S.C. Rand, R.S. Turley, R.A. McFarlane, and O.M. Stafsudd, "High-resolution, nearly-degenerate four-wave mixing in Nd-doped β"-Alumina," International Quantum Electronics Conference (IQEC'87), Baltimore, MD, April 27- May 1.

12. J.F. Lam and S.C. Rand, "Modified dipole-dipole interactions on optically excited pair transitions," International Quantum Electronics Conference (IQEC'87), Baltimore, MD, Apri 27- May 1, 1987 paper MBB6.

13. J.F. Lam, "Four-wave mixing spectroscopy of state-selective collisions in gases and solids," presented at the Third International Laser Science Conference, Atlantic City, N.J., November 1-5, 1987.

14. S.C. Rand, "Ultraviolet phase conjugation with metastable color center states in diamond," Optics Lett. 13 140 1988.

15. R.A. McFarlane, "Dual Wavelength Visible Upconversion Laser," in preparation.

REFERENCES

1. S.A. Pollack and M. Robinson, Electron. Lett. 24, 320 (1988).

2. R.S. Quimby, 5th International Symposium on Halide Glasses, Japan, May 29-June 2, 1988.

3. E.M. Pacheco and C.B. DeAraiyo, Chem. Phys. Lett. 148, 334 (1988).

4. W. Shi, Ph.D. Dissertation, University of Southern California, July 1988.

5. L.F. Johnson and H.J. Guggenheim, Appl. Phys. Lett. 20, 474 (1972).

6. A.J. Silversmith, W. Lenth and R.M. McFarlane, Appl. Phys. Lett. 51, 1977 (1987).